

Quantum optical effective-medium theory for layered metamaterials

Ehsan Amooghorban^{1,2,*} and Martijn Wubs^{3,4,†}

¹*Department of Physics, Faculty of Basic Sciences,
Shahrekord University, P.O. Box 115, Shahrekord 88186-34141, Iran*

²*Photonics Research Group, Shahrekord University, P.O. Box 115, Shahrekord 88186-34141, Iran*

³*Department of Photonics Engineering, Technical University of Denmark, DK-2800 Kgs. Lyngby, Denmark*

⁴*Center for Nanostructured Graphene, Technical University of Denmark, DK-2800 Kgs. Lyngby, Denmark*

(Dated: July 10, 2018)

The quantum optics of metamaterials starts with the question whether the same effective-medium theories apply as in classical optics. In general the answer is negative. For active plasmonics but also for some passive metamaterials, we show that an additional effective-medium parameter is indispensable besides the effective index, namely the effective noise-photon distribution. Only with the extra parameter can one predict how well the quantumness of states of light is preserved in the metamaterial. The fact that the effective index alone is not always sufficient and that one additional effective parameter suffices in the quantum optics of metamaterials is both of fundamental and practical interest. Here from a Lagrangian description of the quantum electrodynamics of media with both linear gain and loss, we compute the effective noise-photon distribution for quantum light propagation in arbitrary directions in layered metamaterials, thereby detailing and generalizing our recent work [E. Amooghorban *et al.*, Phys. Rev. Lett. **110**, 153602 (2013)]. The effective index with its direction and polarization dependence is the same as in classical effective-medium theories. As our main result we derive both for passive and for active media how the value of the effective noise-photon distribution too depends on the polarization and propagation directions of the light. Interestingly, for TE-polarized light incident on passive metamaterials, the noise-photon distribution reduces to a thermal distribution, but for TM-polarized light it does not. We illustrate the robustness of our quantum optical effective-medium theory by accurate predictions both for power spectra and for balanced homodyne detection of output quantum states of the metamaterial.

PACS numbers: 42.50.Ct, 42.50.Nn, 03.70.+k, 78.20.Ci, 78.67.Pt

I. INTRODUCTION

Metamaterials are known and studied for guiding and manipulating light in ways not seen in Nature. [1, 2]. They consist of repeated designed subwavelength unit-cell structures that allow a description of the metamaterial in terms of effective optical parameters not found in natural materials, with negative-index metamaterials [1, 3] as the prime example. In this Introduction we discuss applications of metamaterials in quantum optics, and motivate the need for a quantum optical effective-medium theory.

Applications in optics of metamaterials include flat superlenses [1, 4–6] and sensors [7]. Metamaterials can constitute a material basis for applications of transformation optics [8] such as cloaking devices, which typically require graded-index media realized as graded-*effective*-index media. The properties of a metamaterial derive from an average of its constituting materials, which often involve both metals and dielectrics. There are different ways to determine the effective refractive index of a metamaterial, which is the topic of homogenization theory [9–18].

One important class of structures for which such averaging can produce truly new functionalities are the

epsilon-near-zero (or ENZ) materials [19–22], in which light propagates with extremely small phases and long effective wavelengths, as has been realized also at visible wavelengths [23, 24]. Dispersion-compensated metamaterials can also lead to new devices [25]. Loss-compensated metamaterials constitute another class of structures for which averaging over a unit cell can produce something truly new [4, 26, 27]: loss in one constituent can be compensated by linear gain in another, so as to produce metamaterials with lower or even vanishing effective loss. Partial loss compensation has been realized both in plasmonic waveguides [28, 29] and in metamaterials [30]. Loss compensation is studied in the field of active plasmonics and tuneable metamaterials [31–33]. All mentioned applications of metamaterials are within the realm of classical electromagnetism.

Quantum plasmonics concerns the study of quantum optics with plasmons [34]. It is a stimulating question which of the mentioned applications of metamaterials can be transferred to quantum optics. Indeed an increasing number of researchers is exploring how to manipulate quantum emitters and quantum states of light using metamaterials [35–43]. Vice versa, the exploration how quantum states of light can be used to analyze metamaterial properties has also only just begun [44, 45].

The best known and important example of metamaterials with new functionality for quantum emitters are the hyperbolic metamaterials. Their effective epsilon is positive in one or two directions and negative-valued in the re-

* ehsan.amooghorban@sci.sku.ac.ir

† mwubs@fotonik.dtu.dk

maintaining direction(s) [35]. By taking the usual limit of infinitely small unit cells, the iso-frequency dispersion surfaces of such anisotropic bulk media become hyperbolic, with infinite associated local optical density of states. This nonphysical infinity indicates that the usual idealized description of metamaterials needs improvement for embedded quantum emitters, for example by taking into account the nonlocality of the metallic response [46], or the finite size of either the unit cells [47] or the emitters [48]. Thus quantum emitters embedded inside metamaterials provide a challenge for the effective-medium theories [49].

Quantum optics poses another less known challenge to metamaterials, even when probing metamaterials in the far field and when unit cells are much smaller than the operating wavelength: One can do quantum optical experiments to tell apart two metamaterials even though they have the same shape and the same effective index [45]. In classical electrodynamics this would be impossible, but in quantum optics this may even be possible with normally incident light on simple layered metamaterials [45]. This is because of quantum noise. Quantum mechanics poses a limit to the use of the common effective-index theories.

In principle the ‘quantumness’ of light can survive the propagation through a metamaterial. In general, quantum states of light that propagate through absorbing or amplifying media will be affected by quantum noise associated with the loss [50–54] and gain [55, 56]. This also applies to metamaterials. This does not mean that the concept of the effective index breaks down in quantum optics. On the contrary, in Ref. 45 we presented a quantum optical effective-index theory that accurately describes passive metamaterials and the more exotic metamaterials consisting of alternating layers both with gain. The theory also describes the quantum noise in these metamaterials, and can be seen as a direct extension of the usual effective-index theory.

However, for loss-compensated metamaterials we found that the effective index sometimes underestimates the average quantum noise picked up in a unit cell, because loss can be compensated by gain but quantum noise due to loss cannot be compensated by quantum noise due to gain. Thus effective descriptions of loss-compensated metamaterials based solely on the effective index break down in quantum optics. Nevertheless an accurate quantum optical effective-medium theory of loss-compensated metamaterials is still possible, where besides the usual effective index an additional effective-medium parameter is introduced for loss-compensated metamaterials, namely the effective noise photon distribution [45]. These results were obtained only for normally incident light on multilayer metamaterials.

Here we generalize Ref. [45] in important ways by considering quantum optical effective-medium theories for *three-dimensional* light propagation in layered metamaterials. As is well known in classical optics, TE- and TM-polarized light propagate qualitatively different in a layered medium. Analogously, we will here present sur-

prisingly different effective noise-photon densities for TE- and TM-polarized light. Only for normal incidence will they coincide with each other and with the effective noise-photon density of the one-dimensional theory of Ref. [45]. We also address anew the question whether it is only the loss-compensated metamaterials that require an additional effective-medium parameter.

The paper is organized as follows: In Sec. II, we introduce the field quantization of media with both gain and loss, presenting what we believe is the shortest and simplest route from a Lagrangian to a phenomenological quantum electrodynamics based on the classical Green function. We use these results to derive in Sec. III an input-output relation for planar multilayer dielectrics. Then in Sec. IV we derive a quantum optical effective-index theory, and we test its predicted power spectra in Sec. V. A quantum optical effective-medium theory for both *s*- and *p*-polarized light is introduced in Sec. VI, and tested for the propagation of squeezed states of light through metamaterials in Sec. VII. We end with a discussion and conclusions in Sec. VIII, and an appendix.

II. FIELD QUANTIZATION

With application to loss-compensated metamaterials in mind, here we derive a general expression for the quantized electric field after non-normal propagation through a bounded inhomogeneous dielectric medium that exhibits both loss and gain. Quantum-mechanical theories for electromagnetic wave propagation through lossy [50–52] or amplifying [55, 56] dielectrics have been developed previously. We described media with both gain and loss in Ref. 57, where we used path-integral quantization techniques. Here instead we will not use path integrals and instead we give a simpler quantum electrodynamical description of media with both gain and loss, which is valid for arbitrary dielectric structures, including all non-magnetic metamaterials. The method has the advantage that there is a clear relation between the dielectric function of the dielectric medium and the more microscopic coupling parameters in the Lagrangian. Its specific application to multilayer structures then follows in Sec. III.

The quantum electrodynamics of a linearly lossy dielectric can be described by modeling the medium as a reservoir of three-dimensional harmonic oscillators that interacts with the electromagnetic field [50]. We also allow for the possibility that the medium is linearly amplifying in some finite regions of space, with gain ($\text{Im}[\varepsilon(\omega)] \equiv \varepsilon_1(\omega) < 0$) in one or more finite-frequency windows. Linear gain can be modeled as the coupling of the electromagnetic field to a continuum of inverted harmonic oscillators [58, 59].

We introduce our model for optical media with both gain and loss by first specifying its Lagrangian density in real space [57]

$$\mathcal{L} = \mathcal{L}_{\text{EM}} + \mathcal{L}_e + \mathcal{L}_{\text{int}}, \quad (1)$$

where the first term \mathcal{L}_{EM} has the standard form $\mathcal{L}_{\text{EM}} = \frac{1}{2}\varepsilon_0\mathbf{E}^2(\mathbf{x}, t) - \frac{1}{2\mu_0}\mathbf{B}^2(\mathbf{x}, t)$, describing the free electromagnetic field. There is gauge freedom to write the electric field $\mathbf{E} = -\partial\mathbf{A}/\partial t - \nabla\phi$ and the magnetic field $\mathbf{B} = \nabla \times \mathbf{A}$ in terms of the scalar and vector potentials ϕ and \mathbf{A} . For convenience we choose the Coulomb gauge in which the divergence of the vector potential vanishes by definition. The second term \mathcal{L}_e in Eq. (1) denotes the internal dynamics of the linear medium, which we describe in terms of frequency continua of the harmonic vector field $\mathbf{X}_\omega(\mathbf{x}, t)$ as

$$\mathcal{L}_e = \frac{1}{2} \int_0^\infty d\omega \left[\dot{\mathbf{X}}_\omega^2(\mathbf{x}, t) - \omega^2 \mathbf{X}_\omega^2(\mathbf{x}, t) \right] \text{sgn}[\varepsilon_I(\mathbf{x}, \omega)]. \quad (2)$$

We define the polarization field of the medium as

$$\mathbf{P}(\mathbf{x}, t) = \int_0^\infty d\omega g(\mathbf{x}, \omega) \mathbf{X}_\omega(\mathbf{x}, t), \quad (3)$$

and assume a linear coupling of the electromagnetic field with this field,

$$\mathcal{L}_{\text{int}}(\mathbf{A}, \mathbf{P}, \phi) = \mathbf{A}(\mathbf{x}, t) \cdot \dot{\mathbf{P}}(\mathbf{x}, t) + \phi \nabla \cdot \mathbf{P}. \quad (4)$$

The $g(\mathbf{x}, \omega)$ in Eq. (3) is assumed to be a real-valued scalar coupling function of the electromagnetic field to the spatially inhomogeneous medium. At positions and for frequencies for which $\varepsilon_I(\mathbf{x}, \omega)$ is positive-valued, the medium is lossy and $\mathbf{X}_\omega^2(\mathbf{x}, t)$ is an oscillator to which electromagnetic energy is lost, whereas if $\varepsilon_I(\mathbf{x}, \omega)$ has a negative value, then the medium is amplifying the electromagnetic signal. The latter is modeled with oscillators that are called ‘inverted’ because of the overall minus sign $\text{sgn}[\varepsilon_I(\mathbf{x}, \omega)] = -1$ in the material Lagrangian density Eq. (2). The time derivative of the scalar potential ($\dot{\phi}$) does not appear in the Lagrangian density (1). This implies in the first place that the conjugate momentum associated with the scalar potential ϕ is identically zero. Secondly, the scalar potential (by its Euler-Lagrange equation) can be expressed in terms of other degrees of freedom by Poisson’s equation $\varepsilon_0 \nabla^2 \phi = \nabla \cdot \mathbf{P}$. The solution is $\phi(\mathbf{x}, t) = (4\pi\varepsilon_0)^{-1} \int d\mathbf{x}' \nabla' \cdot \mathbf{P}(\mathbf{x}', t) / |\mathbf{x} - \mathbf{x}'|$. The scalar potential is thereby eliminated, and a reduced Lagrangian is obtained where only the vector potential \mathbf{A} , the harmonic vector field \mathbf{X}_ω and their time derivatives appear. To this end, the free electromagnetic field part and its interaction part are rewritten as

$$\mathcal{L}_{\text{EM}}(\mathbf{A}) = \frac{1}{2}\varepsilon_0 \dot{\mathbf{A}}^2(\mathbf{x}, t) - \frac{1}{2\mu_0} (\nabla \times \mathbf{A}(\mathbf{x}, t))^2, \quad (5a)$$

$$\mathcal{L}_{\text{int}}(\mathbf{A}, \mathbf{P}) = \mathbf{A}(\mathbf{x}, t) \cdot \dot{\mathbf{P}}(\mathbf{x}, t) + \frac{1}{8\pi\varepsilon_0} \int d\mathbf{x}' \frac{\nabla \cdot \mathbf{P}(\mathbf{x}, t) \nabla' \cdot \mathbf{P}(\mathbf{x}', t)}{|\mathbf{x} - \mathbf{x}'|}, \quad (5b)$$

while the material Lagrangian density (2) stays without any changes because there is no term including the scalar potential ϕ . Here and in the following we take the medium to be non-magnetic, and for extensions to magnetodielectrics we refer to Ref. 57. The Lagrangian (1),

with the vector potential \mathbf{A} , and the continua of the polarization operator \mathbf{X}_ω can be used as canonical fields with the following corresponding canonically conjugate fields

$$-\varepsilon_0 \mathbf{E}(\mathbf{x}, t) \equiv \frac{\delta \mathcal{L}}{\delta \dot{\mathbf{A}}(\mathbf{x}, t)} = \varepsilon_0 \dot{\mathbf{A}}(\mathbf{x}, t), \quad (6a)$$

$$\begin{aligned} \mathbf{Q}_\omega(\mathbf{x}, t) &\equiv \frac{\delta \mathcal{L}}{\delta \dot{\mathbf{X}}_\omega(\mathbf{x}, t)} \\ &= g(\omega, \mathbf{x}) \mathbf{A}(\mathbf{x}, t) + \text{sgn}[\varepsilon_I(\mathbf{x}, \omega)] \dot{\mathbf{X}}_\omega(\mathbf{x}, t). \end{aligned} \quad (6b)$$

Until now there is no difference with a classical description. We arrive at a quantum theory by taking the fields to be quantum fields (operator vector fields) that satisfy non-vanishing equal-time commutation relations with their canonically conjugate fields. Apart from the subtlety with the sign functions in Eq. (6c) that discriminate between the frequency intervals where there is gain and loss, this canonical quantization of the fields can proceed in a standard fashion by demanding equal-time commutation relations

$$[A_i(\mathbf{x}, t), -\varepsilon_0 E_j(\mathbf{x}', t)] = i\hbar \delta_{ij} \delta^\perp(\mathbf{x} - \mathbf{x}'), \quad (7a)$$

$$[X_{\omega,i}(\mathbf{x}, t), Q_{\omega',j}(\mathbf{x}', t)] = i\hbar \delta_{ij} \delta(\omega - \omega') \delta^3(\mathbf{x} - \mathbf{x}'), \quad (7b)$$

while all other equal-time commutators vanish. Using the Lagrangian (1) and the expression for the canonical conjugate variables in Eq. (6), we obtain the Hamiltonian density

$$\begin{aligned} \mathcal{H}(\mathbf{x}, t) &= \frac{1}{2}\varepsilon_0 \mathbf{E}^2(\mathbf{x}, t) + \frac{\mathbf{B}^2(\mathbf{x}, t)}{2\mu_0} \\ &+ \frac{1}{2} \int_0^\infty d\omega \text{sgn}[\varepsilon_I(\mathbf{x}, \omega)] \\ &\times \{ (\mathbf{Q}_\omega(\mathbf{x}, t) - g(\omega, \mathbf{x}) \mathbf{A}(\mathbf{x}, t))^2 + \omega^2 \mathbf{X}_\omega^2(\mathbf{x}, t) \}. \end{aligned} \quad (8)$$

Maxwell’s equations can now be obtained from the Heisenberg equations of motion for the vector potential and the transverse electric field and from the commutation relation Eq. (7),

$$\dot{\mathbf{A}}(\mathbf{x}, t) = -\mathbf{E}(\mathbf{x}, t), \quad (9a)$$

$$\varepsilon_0 \dot{\mathbf{E}}(\mathbf{x}, t) = \mu_0^{-1} \nabla \times \nabla \times \mathbf{A}(\mathbf{x}, t) - \dot{\mathbf{P}}(\mathbf{x}, t). \quad (9b)$$

Using the definitions $\mathbf{D} = \varepsilon_0 \mathbf{E} + \mathbf{P}$ for the displacement field and $\mathbf{H} = \mathbf{B}/\mu_0$ for the magnetic field strength, Eqs. (9) result in $\dot{\mathbf{D}}(\mathbf{x}, t) = \nabla \times \mathbf{H}(\mathbf{x}, t)$ and $\dot{\mathbf{B}}(\mathbf{x}, t) = -\nabla \times \mathbf{E}(\mathbf{x}, t)$, showing the consistency with Maxwell’s equations. In a similar fashion, the Heisenberg equation of motion for the dynamical variable \mathbf{X}_ω leads to the second-order differential equation

$$\ddot{\mathbf{X}}_\omega(\mathbf{x}, t) = -\omega^2 \mathbf{X}_\omega(\mathbf{x}, t) + \text{sgn}[\varepsilon_I(\omega)] g(\mathbf{x}, \omega) \mathbf{E}(\mathbf{x}, t), \quad (10)$$

which has the formal solution

$$\begin{aligned} \mathbf{X}_\omega(\mathbf{x}, t) &= \left(\dot{\mathbf{X}}_\omega(\mathbf{x}, 0) \frac{\sin \omega t}{\omega} + \mathbf{X}_\omega(\mathbf{x}, 0) \cos \omega t \right) \\ &+ g(\mathbf{x}, \omega) \text{sgn}[\varepsilon_I(\mathbf{x}, \omega)] \int_0^t dt' \frac{\sin \omega(t-t')}{\omega} \mathbf{E}(\mathbf{x}, t'). \end{aligned} \quad (11)$$

In classical electrodynamics, one would typically assume the corresponding initial fields $\dot{\mathbf{X}}_\omega(\mathbf{x}, 0)$ and $\mathbf{X}_\omega(\mathbf{x}, 0)$ to vanish, which is something that one should not do for the initial quantum operators in Eq. (11) if only because this would violate their commutation relations. It is these initial-operator terms in Eq. (11) that give rise to the qualitatively new phenomenon of quantum noise, as we shall see shortly.

To facilitate our further calculations, let us introduce the annihilation operator

$$d_j(\mathbf{x}, \omega, t) = \frac{1}{\sqrt{2\hbar\omega}} [-i\omega X_{\omega,j}(\mathbf{x}, t) + Q_{\omega,j}(\mathbf{x}, t)], \quad (12)$$

where $j = 1, 2, 3$ labels the three orthogonal spatial directions. Their commutation relations follow immediately from Eq. (7),

$$[d_j(\mathbf{x}, \omega, t), d_{j'}^\dagger(\mathbf{x}', \omega', t)] = \delta_{jj'} \delta(\omega - \omega') \delta^3(\mathbf{x} - \mathbf{x}') \quad (13)$$

Now by inverting the relations (12) and substituting the result into Eq. (3), the polarization field of the medium can be written in terms of creation and annihilation operators as

$$\mathbf{P}(\mathbf{x}, t) = \varepsilon_0 \int_0^\infty dt' \chi(\mathbf{x}, t - t') \mathbf{E}(\mathbf{x}, t') + \mathbf{P}^N(\mathbf{x}, t). \quad (14)$$

Here, the time-dependent susceptibility is defined as

$$\chi(\mathbf{x}, t) = \frac{\Theta(t)}{\varepsilon_0} \int_0^\infty d\omega \operatorname{sgn}[\varepsilon_1(\mathbf{x}, \omega)] g^2(\mathbf{x}, \omega) \frac{\sin \omega t}{\omega}, \quad (15)$$

which is a causal response function because of the step function $\Theta(t)$. After Fourier transformation, the susceptibility becomes

$$\chi(\mathbf{x}, \omega) = \frac{1}{\varepsilon_0} \int_0^\infty d\omega' \frac{g^2(\mathbf{x}, \omega') \operatorname{sgn}[\varepsilon_1(\mathbf{x}, \omega')]}{\omega'^2 - (\omega + i0^+)^2}. \quad (16)$$

The field $\mathbf{P}^N(\mathbf{x}, t)$ in Eq. (14) is the electric polarization noise density that is inevitably associated with absorption and amplification inside medium. As in the phenomenological method of Refs. 55 and 56, we can separate this noise operator into positive- and negative-frequency parts $\mathbf{P}^N = \mathbf{P}^{N(+)} + \mathbf{P}^{N(-)}$ with $\mathbf{P}^{N(-)} = [\mathbf{P}^{N(+)}]^\dagger$, where

$$P_i^{N(+)}(\mathbf{x}, t) = i \int_0^\infty d\omega \sqrt{\frac{\hbar\varepsilon_0 |\varepsilon_1(\mathbf{x}, \omega)|}{|\varepsilon_1(\mathbf{x}, \omega)|}} \pi f_i(\mathbf{x}, \omega) e^{-i\omega t}, \quad (17)$$

in terms of the operator $f_i(\mathbf{x}, \omega)$ that has the form $d_i(\mathbf{x}, \omega, 0)\Theta[\varepsilon_1(\mathbf{x}, \omega)] + d_i^\dagger(\mathbf{x}, \omega, 0)\Theta[-\varepsilon_1(\mathbf{x}, \omega)]$. This noise operator is indeed expressed in terms of material operators at the initial time $t = 0$, as anticipated. If we now take the time derivative of Maxwell's equations in Eq. (9) and insert Eq. (14), then we obtain the frequency-domain wave equation for the positive-frequency part of the vector potential

$$\nabla \times \nabla \times \mathbf{A}^{(+)} - \frac{\omega^2}{c^2} \varepsilon \mathbf{A}^{(+)} = -i\mu_0 \omega \mathbf{P}^{N(+)}, \quad (18)$$

where the electric permittivity $\varepsilon(\mathbf{x}, \omega) = 1 + \chi(\mathbf{x}, \omega)$ satisfies the Kramers-Kronig relations because $\chi(\mathbf{x}, t)$ in Eq. (15) vanishes for $t < 0$. Furthermore, the noise operator $\mathbf{P}^{N(+)}(\mathbf{x}, \omega)$ in the wave equation (18) plays the role of a Langevin force associated with the quantum noise sources in the dielectric. This equation can be solved as

$$\begin{aligned} \mathbf{A}^{(+)}(\mathbf{x}, t) &= \frac{-i\mu_0}{\sqrt{2\pi}} \int_0^\infty d\omega \omega \int d^3\mathbf{x}' \\ &\quad \times \mathbf{G}(\mathbf{x}, \mathbf{x}', \omega) \cdot \mathbf{P}^{N(+)}(\mathbf{x}', \omega) e^{-i\omega t} \\ &= \int_0^\infty d\omega \int d^3\mathbf{x}' \sqrt{\frac{\hbar\mu_0\omega^2 |\varepsilon_1(\mathbf{x}', \omega)|}{\pi c^2}} \\ &\quad \times \mathbf{G}(\mathbf{x}, \mathbf{x}', \omega) \cdot \mathbf{f}(\mathbf{x}', \omega) e^{-i\omega t}, \end{aligned} \quad (19)$$

where $\mathbf{G}(\mathbf{x}, \mathbf{x}', \omega)$ is the classical causal Green function (a tensor) that is defined by the equation

$$\left[\nabla \times \nabla \times - \frac{\omega^2}{c^2} \varepsilon(\mathbf{x}, \omega) \right] \mathbf{G}(\mathbf{x}, \mathbf{x}', \omega) = \delta^3(\mathbf{x} - \mathbf{x}') \mathbf{1}_3. \quad (20)$$

From our Lagrangian theory we thus arrive at the following more phenomenological quantum theory of light in a medium with loss and gain: given a dielectric function $\varepsilon(\mathbf{x}, \omega)$, compute the classical Green function (20) and use this to determine the vector potential (19). With Maxwell's equations all other fields can then also be determined.

III. INPUT-OUTPUT RELATION FOR PLANAR DIELECTRICS

Let us now specify that the dielectric medium with loss and/or gain is a planar dielectric for which the dielectric function $\varepsilon(\mathbf{x}, \omega)$ varies in a step-wise fashion in the z -direction, as depicted in Fig. 1. Main goal of this paper is proposing and testing effective-medium theories that are accurate in quantum optics. The test consists of a comparison between an exact formalism for quantum optics in multilayer media on the one hand and effective descriptions for planar metamaterials on the other. In this section we will derive the mentioned exact formalism, while the numerical comparison will be made in Sec. IV.

We look for a quantum optical input-output relation that can describe the action of a lossy and / or linearly amplifying multilayer medium on an arbitrary quantum state of light incoming from an arbitrary direction with either s - or p -polarization. The sought input-output relation is an operator relation, relating the (annihilation) operators describing the incoming light to the annihilation operators of the outgoing light. To this end, more is needed than just the classical scattering matrix of a multilayer medium, because the incoming quantum state of light is not the only source that determines the output radiation. Quantum noise photons in the lossy and amplifying layers constitutes another source.

The classical Green function plays a central role, describing both the propagation of the incoming light and of

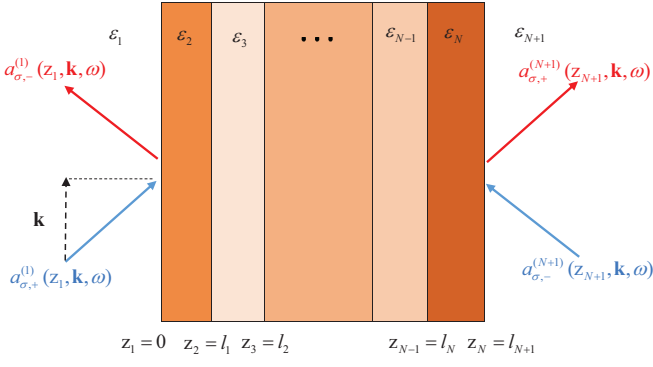


FIG. 1. (Color online) Sketch of the planar dielectric medium with permittivity $\varepsilon_j(\omega)$ and thickness l_j of the j^{th} layer. The arrows denote incoming and outgoing fields. Also shown are the corresponding annihilation operators used in the definitions of the electric-field operator Eq. (28).

the quantum noise photons towards the output direction or detector. As a generalization of the result by Tomáš for lossy dielectric multilayers [60], we already derived the Green function for multilayer media with both lossy

and amplifying layers in Ref. 57, and we will make use of that result here. We will then show in more detail that the explicit form of that Green function allows a suitable rewriting of the vector potential in Eq. (19) as the sought operator input-output relation. We will thereby arrive at a gain-and-loss-in-3D generalization of the 1D-formalism by Gruner *et al.* who studied the QED only of lossy planar dielectrics [52]. In our notation we follow Ref. [60].

Multilayer media (see illustration in Fig. 1) are translationally invariant in two spatial directions. It is often convenient to exploit this symmetry by introducing the transverse spatial Fourier transform in the directions of translational invariance,

$$\mathbf{G}(\mathbf{x}, \mathbf{x}', \omega) = \frac{1}{2\pi} \int d^2\mathbf{k} e^{i\mathbf{k}\cdot(\boldsymbol{\rho}-\boldsymbol{\rho}')} \mathbf{G}(\mathbf{k}, z, z', \omega) \quad (21)$$

where \mathbf{k} is a two-dimensional vector in the x, y -subspace and $\boldsymbol{\rho} = (x, y)$. The Green tensor $\mathbf{G}(\mathbf{k}, z, z', \omega)$ assumes two different forms, depending on whether z and z' are located in the same layer or not. For z' in layer j it is given by [57, 60]

$$\mathbf{G}(\mathbf{k}, z, z', \omega) = \frac{1}{2\pi\varepsilon_0\varepsilon_j(\omega)\omega^2} \delta(z - z') \hat{z}\hat{z} + \frac{1}{4\pi\beta_j} \sum_{\sigma=s}^p \xi_\sigma \frac{e^{-\beta_j l_j}}{D_\sigma^j} \times [\mathcal{E}_{\sigma>}^{(j)}(\mathbf{k}, \omega; z) \mathcal{E}_{\sigma<}^{(j)}(-\mathbf{k}, \omega; z') \Theta(z - z') + \mathcal{E}_{\sigma<}^{(j)}(\mathbf{k}, \omega; z) \mathcal{E}_{\sigma>}^{(j)}(-\mathbf{k}, \omega; z') \Theta(z' - z)], \quad z \text{ also in layer } j \quad (22a)$$

$$\mathbf{G}(\mathbf{k}, z, z', \omega) = \frac{1}{4\pi\beta_n} \sum_{\sigma=s}^p \xi_\sigma \frac{t_\sigma^{n/j} e^{-(\beta_j l_j + \beta_n l_n)}}{D_\sigma^j} \times \left[\frac{\mathcal{E}_{\sigma>}^{(n)}(\mathbf{k}, \omega; z)}{D_{\sigma,+}^{n/j}} \mathcal{E}_{\sigma<}^{(j)}(-\mathbf{k}, \omega; z') \Theta(n - j) + \frac{\mathcal{E}_{\sigma<}^{(n)}(\mathbf{k}, \omega; z)}{D_{\sigma,-}^{n/j}} \mathcal{E}_j^{\sigma>}(-\mathbf{k}, \omega; z') \Theta(j - n) \right], \quad z \text{ in layer } n \neq j \quad (22b)$$

where $\xi_s = -1$, $\xi_p = 1$, and $\Theta(z)$ is the usual unit step function, and

$$\mathcal{E}_{\sigma>}^{(j)}(\mathbf{k}, \omega; z) = \mathbf{e}_{\sigma,+}^{(j)}(\mathbf{q}) e^{-\beta_j(z-d_j)} + r_{j+}^\sigma \mathbf{e}_{\sigma,-}^{(j)}(\mathbf{k}) e^{\beta_j(z-d_j)}, \quad (23a)$$

$$\mathcal{E}_{\sigma<}^{(j)}(\mathbf{k}, \omega; z) = \mathbf{e}_{\sigma,-}^{(j)}(\mathbf{k}) e^{\beta_j z} + r_{j-}^\sigma \mathbf{e}_{\sigma,+}^{(j)} + (\mathbf{k}) e^{-\beta_j z}. \quad (23b)$$

Here σ stands for s - or p -polarization, and $\mathbf{e}_{s,\pm}^{(j)} = (\hat{\mathbf{k}} \times \hat{z})$ and $\mathbf{e}_{p,\pm}^{(j)} = \frac{-1}{k_j} (|\mathbf{k}\hat{z} \pm \beta_j \hat{\mathbf{k}})$ are the polarization vectors for s - and p -polarized waves propagating in the positive/negative- z direction, with $k_j \equiv \sqrt{\omega^2 \varepsilon_j(\omega)/c^2} = k_j' + i k_j''$ and

$$\beta_j(\mathbf{k}, \omega) = \sqrt{\varepsilon_j(\omega)\omega^2/c^2 - \mathbf{k}^2} = \beta_j' + i\beta_j'' \quad (24)$$

is the normal component of the wave vector in layer j^{th} and \mathbf{k} the in-plane wave vector. Other quantities

in Eqs. (22) that still need to be defined are

$$D_\sigma^j = 1 - r_{\sigma,-}^{(j)} r_{\sigma,+}^{(j)} e^{-2\beta_j l_j}, \quad (25a)$$

$$D_{\sigma,\pm}^{n/j} = 1 - r_{\sigma,\pm}^{(n)} r_{\sigma,\mp}^{n-1/j} e^{-2\beta_n l_n}, \quad (25b)$$

where $r_{\sigma,-}^{(j)}$ and $r_{\sigma,+}^{(j)}$ are the Fresnel coefficients for reflection at the left/right boundary of layer j . In addition, $t_\sigma^{n/j}$ and $r_\sigma^{n/j}$ are the transmission and reflection coefficients between the layers n and j .

The Green function (22) is hereby defined, but not yet automatically well-defined: it is a known issue that the normal component of the wave vector Eq. (24) for active multilayer media is not automatically well defined even if the refractive index is well-defined: although the refractive index has no branch points in the upper half-plane because of causality, $\beta_j(\mathbf{k}, \omega)$ may have branch points there [61]. If so, then $\beta_j(\mathbf{q}, \omega)$ loses its usual physical interpretation as the propagation constant in the normal direction, since waves propagating perpendicularly to the

z -axis propagate an infinite distance, and therefore pick up an infinite amount of gain, before arriving at any other plane $z = \text{const}$. This instability could be eliminated by limiting the extent of the active medium in the transverse direction. We will follow instead Refs. [61–63] and only consider active media without branch points where $\beta_j(\omega)$ is meaningful for real frequencies. In that case the signs of β'_j and β''_j are identical to those of $\text{Re}[\varepsilon_j(\omega)]$ and $\text{Im}[\varepsilon_j(\omega)]$, respectively (see Refs. [61–63]).

We will now use this Green tensor (22) to write the electric-field operator (19) in terms of creation and annihilation operators for which we will then identify input-output relations. Expressed in the same mixed Fourier representation as for the Green function, the electric-field operator becomes

$$\mathbf{E}^{(j)}(\mathbf{x}, t) = \frac{1}{(2\pi)^{3/2}} \int d^2\mathbf{k} \int d\omega \left[e^{i(\mathbf{k}\cdot\boldsymbol{\rho} - \omega t)} \mathbf{E}^{(j)}(z, \mathbf{k}, \omega) + h.c. \right], \quad (26)$$

where the electric-field component

$$\mathbf{E}^{(j)}(z, \mathbf{k}, \omega) = \sum_{\sigma=p,s} \left[E_{\sigma,+}^{(j)}(z, \mathbf{k}, \omega) \mathbf{e}_{\sigma,+}^{(j)}(\mathbf{k}) + E_{\sigma,-}^{(j)}(z, \mathbf{k}, \omega) \mathbf{e}_{\sigma,-}^{(j)}(\mathbf{k}) \right], \quad (27)$$

is associated with light propagation both to the right (+) and left (-). These ‘amplitudes’ $E_{\sigma,\pm}^{(j)}(z, \mathbf{k}, \omega)$ associated with right-and left propagation inside the j th layer can be written in terms of amplitude operators $a_{\sigma,\pm}^{(j)}(z, \mathbf{k}, \omega)$ as

$$E_{\sigma,\pm}^{(j)}(z, \mathbf{k}, \omega) = \frac{i\omega}{\beta_j c} \sqrt{\frac{\hbar\beta'_j}{2\varepsilon_0}} e^{\pm i\beta'_j z} a_{\sigma,\pm}^{(j)}(z, \mathbf{k}, \omega), \quad (28)$$

where the z -dependence of the amplitude operators $a_{\sigma,\pm}^{(j)}(z, \mathbf{k}, \omega)$ is governed by quantum Langevin equations

$$\frac{\partial a_{\sigma,\pm}^{(j)}(z, \mathbf{k}, \omega)}{\partial z} = \mp \beta''_j a_{\sigma,\pm}^{(j)}(z, \mathbf{k}, \omega) \pm \frac{\sqrt{2|\beta''_j|}}{i} e^{\mp i\beta'_j z} f_{\sigma,\pm}^{(j)}(z, \mathbf{k}, \omega), \quad (29)$$

so that the operators $a_{\sigma,\pm}^{(j)}(z, \mathbf{k}, \omega)$ and $a_{\sigma,\pm}^{(j)}(z', \mathbf{k}, \omega)$ for different space points within the same j th layer are related as

$$a_{\sigma,\pm}^{(j)}(z, \mathbf{k}, \omega) = e^{\mp \beta''_j(z-z')} a_{\sigma,\pm}^{(j)}(z', \mathbf{k}, \omega) \pm \frac{\sqrt{2|\beta''_j|}}{i} e^{\mp \beta'_j z} \times \int_{z'}^z dz'' e^{\mp i\beta'_j z''} f_{\sigma,\pm}^{(j)}(z'', \mathbf{k}, \omega). \quad (30)$$

Here the $f_{\sigma,\pm}^{(j)}(\pm z', \mathbf{k}, \omega) = \mathbf{f}^{(j)}(\pm z', \mathbf{k}, \omega) \cdot \mathbf{e}_{\sigma,\pm}^{(j)}(\mathbf{k})$ are bosonic field operators that play the role of fundamental variables of the electromagnetic field and medium, and $\mathbf{f}^{(j)}(\pm z', \mathbf{k}, \omega)$ is the partial Fourier transform of $\mathbf{f}(\mathbf{x}, \omega)$

in layer j of Eq. (19). They satisfy the commutation relations

$$\left[f_{\sigma,\pm}^{(j)}(z, \mathbf{k}, \omega), f_{\sigma',\pm}^{(j)\dagger}(z', \mathbf{k}', \omega') \right] = \varrho_{\sigma,+}^{(j)} \text{sgn}[\varepsilon_{1j}(\omega)] \delta_{jj'} \delta_{\sigma\sigma'} \times \delta(z-z') \delta(\omega-\omega') \delta(\mathbf{k}-\mathbf{k}'), \quad (31a)$$

$$\left[f_{\sigma,\pm}^{(j)}(z, \mathbf{k}, \omega), f_{\sigma',\mp}^{(j)\dagger}(z', \mathbf{k}', \omega') \right] = \varrho_{\sigma,-}^{(j)} \text{sgn}[\varepsilon_{1j}(\omega)] \delta_{jj'} \delta_{\sigma\sigma'} \times \delta(z-z') \delta(\omega-\omega') \delta(\mathbf{k}-\mathbf{k}'), \quad (31b)$$

Here, the coefficient $\rho_{\sigma,\pm}^{(j)}$ is defined to be equal to unity for s -polarization (i.e. for $\sigma = s$), while it is equal to $(\mathbf{k}^2 \pm |\beta_j|^2)/|k_j|^2$ for $\sigma = p$. Notice that the plus and minus subscripts in this coefficient $\rho_{\sigma,\pm}^{(j)}$ do not correspond to a propagation direction, but rather to two identical (+) and opposite (-) propagation directions.

Combining Eqs. (26) and (27) together with Eqs. (28) and (30), the electric-field operator for the j th layer may be represented in a convenient form as

$$\mathbf{E}^{(j)}(\mathbf{x}, t) = \frac{1}{2\pi} \sum_{\sigma} \int d^2\mathbf{k} \int_0^{\infty} d\omega \left[\frac{-i\omega}{2\beta_j c} \sqrt{\frac{\hbar\beta'_j}{\pi\varepsilon_0}} e^{i(\mathbf{k}\cdot\boldsymbol{\rho} - \omega t)} \times \left(e^{i\beta'_j z} a_{\sigma,+}^{(j)}(z, \mathbf{k}, \omega) \mathbf{e}_{\sigma,+}^{(j)}(\mathbf{k}) + e^{-i\beta'_j z} a_{\sigma,-}^{(j)}(z, \mathbf{k}, \omega) \mathbf{e}_{\sigma,-}^{(j)}(\mathbf{k}) \right) + h.c. \right], \quad (32)$$

where the properties of the amplitude operators have now been established. It is worth mentioning that an ordinary normal-mode expansion for the electric-field operator is recovered from this equation for frequencies ω far from the resonances of the medium: when gain and loss may be disregarded, i.e. in the limit $\varepsilon_{1j}(\omega) \rightarrow 0$, the operators $a_{\sigma,\pm}^{(j)}(z, \mathbf{k}, \omega)$ become mode operators independent of z .

These equations (26)–(32) will make it possible to calculate the input and output fields at any position outside the multilayer medium recursively, without explicitly applying the multilayer Green function (22). We derive this recursive procedure in three steps: first, within each layer j we relate the amplitude operators on the extreme left and right to each other, i.e. at the positions $z = z_{j-1}$ and at $z = z_j$. Second, we relate the operators in neighboring layers across an interface. Third, by making repeated use of the previous two steps, we can relate the amplitude operators $a_{\sigma,-}^{(1)}(z, \mathbf{k}, \omega)$ and $a_{\sigma,+}^{(N+1)}(z, \mathbf{k}, \omega)$ for the outgoing fields to the left and right of the multilayered, respectively, to the operators of the corresponding incoming fields, $a_{\sigma,+}^{(1)}(z, \mathbf{k}, \omega)$ and $a_{\sigma,-}^{(N+1)}(z, \mathbf{k}, \omega)$, and the noise operators. We discuss these three steps in some more detail below.

Step 1.— The first step is readily found by realizing

that Eq. (30) for $z = z_j$ can be written in matrix form as

$$\begin{pmatrix} a_{\sigma,+}^{(j)}(z_j, \mathbf{k}, \omega) \\ a_{\sigma,-}^{(j)}(z_j, \mathbf{k}, \omega) \end{pmatrix} = R_{\sigma}^{(j)} \begin{pmatrix} a_{\sigma,+}^{(j)}(z_{j-1}, \mathbf{k}, \omega) \\ a_{\sigma,-}^{(j)}(z_{j-1}, \mathbf{k}, \omega) \end{pmatrix} + \begin{pmatrix} c_{\sigma,+}^{(j)}(\mathbf{k}, \omega) \\ c_{\sigma,-}^{(j)}(\mathbf{k}, \omega) \end{pmatrix} \quad (33)$$

where $R_{\sigma}^{(j)}$ is a diagonal 2×2 matrix with $R_{\sigma,11}^{(j)} = 1/R_{\sigma,22}^{(j)} = e^{-\beta_j'' l_j}$. The quantum noise operators in this matrix equation (33) are given by

$$c_{\sigma,\pm}^{(j)}(\mathbf{k}, \omega) = \pm \frac{\sqrt{2|\beta_j''|}}{i} e^{\mp \beta_j'' z_j} \times \int_{z_{j-1}}^{z_j} dz' e^{\mp i \beta_j'' z'} f_{\sigma,\pm}^{(j)}(z', \mathbf{k}, \omega), \quad (34)$$

and evidently these inhomogeneous terms in the matrix relation (33) are the qualitative novelty as compared to the standard transfer-matrix analysis of multilayer media in classical electrodynamics. Recalling the commutation relations (31), the operators $c_{\sigma,\pm}^{(j)}(\mathbf{k}, \omega)$ are found to satisfy the commutation relations

$$\begin{aligned} [c_{\sigma,\pm}^{(j)}(\mathbf{k}, \omega), c_{\sigma',\pm}^{(j)\dagger}(\mathbf{k}', \omega')] &= 2 \rho_{\sigma,+}^{(j)} e^{\mp \beta_j'' l_j} \sinh(\beta_j'' l_j) \delta_{\sigma\sigma'} \\ &\times \delta(\omega - \omega') \delta^2(\mathbf{k} - \mathbf{k}'), \end{aligned} \quad (35a)$$

$$\begin{aligned} [c_{\sigma,\pm}^{(j)}(\mathbf{k}, \omega), c_{\sigma',\mp}^{(j)\dagger}(\mathbf{k}', \omega')] &= -\frac{2\beta_j''}{\beta_j'} \rho_{\sigma,-}^{(j)} e^{\mp i \beta_j'' (z_j + z_{j-1})} \\ &\times \sin(\beta_j'' l_j) \delta_{\sigma\sigma'} \delta(\omega - \omega') \delta^2(\mathbf{k} - \mathbf{k}'). \end{aligned} \quad (35b)$$

Step 2.— In the second step, we relate the operators $a_{\sigma,\pm}^{(j+1)}(z_j, \mathbf{k}, \omega)$ and $a_{\sigma,\pm}^{(j)}(z_j, \mathbf{k}, \omega)$ in neighboring layers across the interface at z_j to each other by using the form Eq. (22c) for the Green function $\mathbf{G}(\mathbf{k}, z, z', \omega)$ for positions z, z' in neighboring layers. This Green function already by construction respects the Maxwell boundary conditions that the tangential components of the electric and magnetic fields be continuous. We obtain the operator matrix relation

$$\begin{pmatrix} a_{\sigma,+}^{(j+1)}(z_j, \mathbf{k}, \omega) \\ a_{\sigma,-}^{(j+1)}(z_j, \mathbf{k}, \omega) \end{pmatrix} = S_{\sigma}^{(j)} \begin{pmatrix} a_{\sigma,+}^{(j)}(z_j, \mathbf{k}, \omega) \\ a_{\sigma,-}^{(j)}(z_j, \mathbf{k}, \omega) \end{pmatrix}, \quad (36)$$

which also holds for classical amplitudes and where the matrix $S_{\sigma}^{(j)}$ is given by

$$S_{\sigma}^{(j)} = \frac{1}{2\beta_j} \sqrt{\frac{\beta_j'}{\beta_{j+1}'}} \begin{pmatrix} (\beta_{j+1} \kappa_{\sigma,j/j+1} + \beta_j \kappa_{\sigma,j+1/j}) e^{i(\beta_j' - \beta_{j+1}') z_j} & (\beta_{j+1} \kappa_{\sigma,j/j+1} - \beta_j \kappa_{\sigma,j+1/j}) e^{-i(\beta_j' + \beta_{j+1}') z_j} \\ (\beta_{j+1} \kappa_{\sigma,j/j+1} - \beta_j \kappa_{\sigma,j+1/j}) e^{i(\beta_j' + \beta_{j+1}') z_j} & (\beta_{j+1} \kappa_{\sigma,j/j+1} + \beta_j \kappa_{\sigma,j+1/j}) e^{-i(\beta_j' - \beta_{j+1}') z_j} \end{pmatrix}, \quad (37)$$

in which $\kappa_{s,j/j+1} = 1$ and $\kappa_{p,j/j+1} = k_j/k_{j-1}$.

Step 3.— In the third, final step, we invoke Eqs. (33) and (36) alternately and repeatedly, until we finally obtain the operator of the outgoing fields to the leftmost and rightmost layers, respectively, $a_{\sigma,-}^{(1)}(z_1, \mathbf{k}, \omega)$ and $a_{\sigma,+}^{(N+1)}(z_N, \mathbf{k}, \omega)$, in terms of the two incoming fields $a_{\sigma,+}^{(1)}(z_1, \mathbf{k}, \omega)$ and $a_{\sigma,-}^{(N+1)}(z_N, \mathbf{k}, \omega)$, as well as the noise fields. The sought input-output relation for amplitude operators is thereby obtained as

$$\begin{pmatrix} a_{\sigma,-}^{(1)}(z_1) \\ a_{\sigma,+}^{(N+1)}(z_N) \end{pmatrix} = \mathcal{A}_{\sigma} \begin{pmatrix} a_{\sigma,+}^{(1)}(z_1) \\ a_{\sigma,-}^{(N+1)}(z_N) \end{pmatrix} + \begin{pmatrix} F_{\sigma,-} \\ F_{\sigma,+} \end{pmatrix}, \quad (38)$$

where we suppressed the (\mathbf{k}, ω) -dependence, and where the quantum noise originating from all layers with either loss or gain is given by

$$\begin{pmatrix} F_{\sigma,-} \\ F_{\sigma,+} \end{pmatrix} = \mathcal{B}_{\sigma}^{(2)} \begin{pmatrix} c_{\sigma,+}^{(2)} \\ c_{\sigma,-}^{(2)} \end{pmatrix} + \dots + \mathcal{B}_{\sigma}^{(N)} \begin{pmatrix} c_{\sigma,+}^{(N)} \\ c_{\sigma,-}^{(N)} \end{pmatrix}, \quad (39)$$

in which the coefficient matrices \mathcal{A}_{σ} and \mathcal{B}_{σ} are given by

$$\mathcal{A}_{\sigma} = A_{\sigma 22}^{-1} \begin{pmatrix} -A_{\sigma 21} & 1 \\ A_{\sigma 11} A_{\sigma 22} - A_{\sigma 12} A_{\sigma 21} & A_{\sigma 12} \end{pmatrix}, \quad (40a)$$

$$\begin{aligned} \mathcal{B}_{\sigma}^{(j)} &= A_{\sigma 22}^{-1} \\ &\times \begin{pmatrix} -B_{\sigma 21}^{(j)} & -B_{\sigma 22}^{(j)} \\ B_{\sigma 11}^{(j)} A_{\sigma 22} - A_{\sigma 12} B_{\sigma 21}^{(j)} & B_{\sigma 12}^{(j)} A_{\sigma 22} - A_{\sigma 12} B_{\sigma 22}^{(j)} \end{pmatrix}. \end{aligned} \quad (40b)$$

Here, the matrices $B_\sigma^{(j)}$ satisfy the recursion relations $B_\sigma^{(k-1)} = B_\sigma^{(k)} \cdot R_\sigma^{(k)} \cdot S_\sigma^{(k-1)}$ and $B_\sigma^{(N)} = S_\sigma^{(N)}$, with $k = 3, 4, \dots, N$, and $A_\sigma = B_\sigma^{(2)} \cdot R_\sigma^{(2)} \cdot S_\sigma^{(1)}$. From Eq. (38) we can appreciate that the multiple transmissions and reflections in the multilayer medium of the incident light are described by the same transfer matrices \mathcal{A}_σ as in classical optics, whereas the matrix elements $\mathcal{B}_\sigma^{(j)}$ have no classical analogues, since they describe the propagation of quantum noise that originates from layer j .

Input and output outside the multilayer.— In this article we will mostly focus on the transmitted and reflected output states of light as compared to the optical input states. Let us therefore specify how from the above general formalism the field operators outside of the multilayer structure are obtained. The amplitude operators of the incoming fields $a_{\sigma,+}^{(1)}(z, \mathbf{k}, \omega)$ and $a_{\sigma,-}^{(N+1)}(z, \mathbf{k}, \omega)$ in Eq. (38) are defined within the space intervals $-\infty < z \leq z_1$ and $z_{N+1} \leq z < \infty$, respectively, see the sketch in Fig. 1. The explicit form of these input operators can be obtained with the use of Eq. (30) as

$$a_{\sigma,+}^{(1)}(z, \mathbf{k}, \omega) = \frac{1}{i} \sqrt{2|\beta_1''|} e^{-\beta_1'' z} \times \int_{-\infty}^z dz' e^{-i\beta_1 z'} f_{\sigma,+}^{(1)}(z', \mathbf{k}, \omega), \quad (41a)$$

$$a_{\sigma,-}^{(N+1)}(z, \mathbf{k}, \omega) = \frac{1}{i} \sqrt{2|\beta_{N+1}''|} e^{\beta_{N+1}'' z} \times \int_z^{\infty} dz' e^{i\beta_{N+1} z'} f_{\sigma,-}^{(N+1)}(z', \mathbf{k}, \omega). \quad (41b)$$

Using the above relations (41) and the commutation relation (31), we find that the input operators satisfy the commutation relations

$$\left[a_{\sigma,+}^{(1)}(z, \mathbf{k}, \omega), a_{\sigma',+}^{(1)\dagger}(z', \mathbf{k}', \omega') \right] = \varrho_{\sigma,+}^{(1)} e^{-\beta''|z-z'|} \times \text{sgn}[\varepsilon_{11}(\omega)] \delta_{\sigma\sigma'} \delta(\omega - \omega') \delta(\mathbf{k} - \mathbf{k}'), \quad (42a)$$

and an analogous relation holds for the operators in the other outer layer labeled $N + 1$ on the opposite size of the metamaterial. It also follows that input operators of different outer layers commute,

$$\left[a_{\sigma,+}^{(1)}(z, \mathbf{k}, \omega), a_{\sigma',-}^{(N+1)\dagger}(z', \mathbf{k}', \omega') \right] = 0, \quad (42b)$$

as one would expect for these independent input channels.

The commutation relations for the output amplitude operators $a_{\sigma,-}^{(1)}(z, \mathbf{k}, \omega)$ and $a_{\sigma,+}^{(N+1)}(z, \mathbf{k}, \omega)$ can also be determined. We do not spell them out here, but they can be derived by applying the input-output relation (38) and the commutation relation (42a). Indeed, the input-output relation (38) together with the commutation relations (42a)–(42b), contain all information necessary to transform an arbitrary function of the input-field operators into the corresponding function of the output-field operators. In particular, it enables one to express arbitrary moments and correlations of the outgoing fields in

terms of those of the incoming fields and the quantum-noise excitations in the multilayers. For normal incidence ($\mathbf{k} = 0$), this general input-output relation reduces to the well-known relation given in [52], which we also made use of in our Ref. 45. The somewhat lengthy equations for general multilayers of the present section reduce to a much simpler form when specified for a single layer, as will be done below in Sec. IV.

IV. QUANTUM OPTICAL EFFECTIVE-INDEX THEORY

In Sec. III we presented an input-output formalism for the electromagnetic field operators in arbitrary layered media with gain and loss, including quantum noise terms. So in principle, the problem is solved how output fields depend on the input, also for layered metamaterials: periodic multilayer media with unit cells much smaller than optical wavelengths. However, for these layered metamaterials one can hope that a simpler, effective description as a homogeneous medium is also possible, here in quantum optics just like it is known to be possible in classical optics.

Expressing quantum noise in terms of the effective index presupposes that we know how to determine the effective material parameters of a metamaterial. This has been thoroughly studied (and still is an active field of study) in classical optics [10–14, 16, 17]. The effective index in quantum optics is the same as in classical optics and can be determined using the same methods. We will use and compare two such methods. First, the scattering method by Smith and co-workers [10, 11, 17] boils down to finding the effective index of a homogeneous medium that mimicks best the transmission and reflection off the metamaterial. Second, we use the dispersion method, where effective parameters are obtained from the small- (k, ω) Taylor expansion of the known dispersion relation of periodic multilayer structures. For completeness we briefly present both methods in Appendix A. We will focus on metamaterials with strongly subwavelength unit cells, for which unique effective parameters can be identified, practically independent of the method used to obtain them.

In this section we present a quantum optical effective-index theory. By this we mean an effective-medium theory that describes the metamaterial entirely in terms of its effective index (or equivalently, in terms of its effective dielectric function). In that sense it does not differ from the usual effective theory in classical optics. But it differs from the usual effective-index theories in classical optics because quantum noise is also described. The crucial assumption is that also the quantum noise of the metamaterial can be described solely in terms of its effective dielectric function. The effective-index theory presented in this section concerns three-dimensional light propagation in layered metamaterials, thereby generalizing the effective-index theory of Ref. [45] to arbitrary propaga-

tion directions and for two distinct types of polarization. The accuracy of the effective-index theory will first be tested in calculations of output intensities in Sec. V.

Output operators of a single homogeneous layer.— Assume that we have used either the scattering or the dispersion method to determine the values for the effective dielectric tensor components for our multilayer structure. And assume that in classical optics the entire structure can effectively be described as a single dielectric layer. Then we can also try and apply the elaborate quantum optical input-output formalism of Sec. III to that single effective layer. With the two planar interfaces of the homogenized slab located at $z_1 = 0$ and $z_N = L$, the input-output relation (38) for the single effective layer reduces to the simpler form

$$\begin{pmatrix} a_{\sigma,-}^{(1)}(z_1, \mathbf{k}, \omega) \\ a_{\sigma,+}^{(N+1)}(z_N, \mathbf{k}, \omega) \end{pmatrix} = \mathcal{A}_{\text{eff},\sigma} \begin{pmatrix} a_{\sigma,+}^{(1)}(z_1, \mathbf{k}, \omega) \\ a_{\sigma,-}^{(N+1)}(z_N, \mathbf{k}, \omega) \end{pmatrix} + \begin{pmatrix} F_{\text{eff}\sigma,-}(\mathbf{k}, \omega) \\ F_{\text{eff}\sigma,+}(\mathbf{k}, \omega) \end{pmatrix}, \quad (43)$$

where according to Eq. (40a), the matrix presentation

$$F_{\text{eff},\sigma-}(\mathbf{k}, \omega) = \frac{-2i\beta_0 \sqrt{2\beta'_{\text{eff},\sigma} \beta''_{\text{eff}} / \beta'_0}}{(\beta_{\text{eff},\sigma} + \beta_0)^2 - (\beta_{\text{eff},\sigma} - \beta_0)^2 \exp[2i\beta_{\text{eff}}L]} \left((\beta_{\text{eff},\sigma} - \beta_0) e^{2i\beta_{\text{eff}}d} \int_0^L dz' e^{-i\beta_{\text{eff}}z'} f_{\text{eff}\sigma,+}(z', \mathbf{k}, \omega) + (\beta_{\text{eff},\sigma} + \beta_0) \int_0^L dz' e^{i\beta_{\text{eff}}\omega z'} f_{\text{eff}\sigma,-}(z', \mathbf{k}, \omega) \right), \quad (46a)$$

$$F_{\text{eff},\sigma+}(\mathbf{k}, \omega) = \frac{-2i\beta_0 \sqrt{2\beta'_{\text{eff},\sigma} \beta''_{\text{eff}} / \beta'_0} \exp[i(\beta_{\text{eff}} - \beta_0)L]}{(\beta_{\text{eff},\sigma} + \beta_0)^2 - (\beta_{\text{eff},\sigma} - \beta_0)^2 \exp[2i\beta_{\text{eff}}L]} \left((\beta_{\text{eff},\sigma} + \beta_0) \int_0^L dz' e^{-i\beta_{\text{eff}}z'} f_{\text{eff}\sigma,+}(z', \mathbf{k}, \omega) + (\beta_{\text{eff},\sigma} - \beta_0) \int_0^L dz' e^{i\beta_{\text{eff}}\omega z'} f_{\text{eff}\sigma,-}(z', \mathbf{k}, \omega) \right), \quad (46b)$$

with the commutation relations

$$\begin{aligned} [F_{\text{eff}\sigma,\pm}(\mathbf{k}, \omega), F_{\text{eff}\sigma',\pm}^\dagger(\mathbf{k}', \omega')] &= \quad (47a) \\ (1 - |r_{\text{eff},\sigma}|^2 - |t_{\text{eff},\sigma}|^2) \delta_{\sigma\sigma'} \delta(\mathbf{k} - \mathbf{k}') \delta(\omega - \omega'), \end{aligned}$$

$$\begin{aligned} [F_{\text{eff}\sigma,\pm}(\mathbf{k}, \omega), F_{\text{eff}\sigma',\mp}^\dagger(\mathbf{k}', \omega')] &= \quad (47b) \\ - (r_{\text{eff},\sigma} t_{\text{eff},\sigma}^* + e^{2i\beta_0 d} r_{\text{eff},\sigma}^* t_{\text{eff},\sigma}) \delta_{\sigma\sigma'} \delta(\mathbf{k} - \mathbf{k}') \delta(\omega - \omega'), \end{aligned}$$

in terms of the classical amplitude reflection and transmission amplitudes of Eq. (45). Furthermore, just like for the general multilayer in Sec. III, the optical input operators of the effective slab satisfy the bosonic commutation

$\mathcal{A}_{\text{eff},\sigma}$ is equal to

$$\begin{pmatrix} r_{\text{eff},\sigma} & t_{\text{eff},\sigma} \\ t_{\text{eff},\sigma} & e^{-2i\beta_0 d} r_{\text{eff},\sigma} \end{pmatrix}, \quad (44)$$

and where the effective complex reflection and transmission amplitudes of the homogenized slab are given by the well-known classical expressions

$$r_{\text{eff},\sigma} = \frac{(\beta_{\text{eff},\sigma}^2 - \beta_0^2) (\exp[2i\beta_{\text{eff}}L] - 1)}{(\beta_{\text{eff},\sigma} + \beta_0)^2 - (\beta_{\text{eff},\sigma} - \beta_0)^2 \exp[2i\beta_{\text{eff}}L]} \quad (45a)$$

$$t_{\text{eff},\sigma} = \frac{4\beta_{\text{eff},\sigma}\beta_0 \exp[i(\beta_{\text{eff}} - \beta_0)L]}{(\beta_{\text{eff}} + \beta_0, \sigma)^2 - (\beta_{\text{eff},\sigma} - \beta_0)^2 \exp[2i\beta_{\text{eff}}L]} \quad (45b)$$

Here, $\beta_{\text{eff},\sigma}$ stands for $\beta_{\text{eff},s} = \beta_{\text{eff}}$ and $\beta_{\text{eff},p} = \beta_{\text{eff}}/\varepsilon_{\text{eff}}$. The effective noise operator $F_{\text{eff},\sigma}$ has no classical analogue. It represents the quantum noise associated with loss and gain and combinations thereof inside this effective medium, and in the present effective-index theory its right- (+) and left-going (-) components are given by

relations

$$\begin{aligned} [a_{\sigma,+}^{(1)}(\mathbf{k}, \omega), a_{\sigma',+}^{(1)\dagger}(\mathbf{k}', \omega')] &= [a_{\sigma,-}^{(N+1)}(\mathbf{k}, \omega), a_{\sigma',-}^{(N+1)\dagger}(\mathbf{k}', \omega')] \\ &= \delta_{\sigma\sigma'} \delta(\mathbf{k} - \mathbf{k}') \delta(\omega - \omega'), \quad (48) \end{aligned}$$

since the input operators in free space incident on the slab cannot sense the presence of the effective slab before these input waves arrive at it. It was therefore to be expected (and a consistency test) that the input operators turned out to have the same commutators as the corresponding quantum operators in free space.

Using the previous two commutation relations and the input-output relations (43), the bosonic commutation relations for the output-mode operators $a_{\sigma,-}^{(1)}$ and $a_{\sigma,+}^{(N+1)}$

can then also be obtained,

$$[a_{\sigma,-}^{(1)}(\mathbf{k}, \omega), a_{\sigma',-}^{(1)\dagger}(\mathbf{k}', \omega')] = [a_{\sigma,+}^{(N+1)}(\mathbf{k}, \omega), a_{\sigma',+}^{(N+1)\dagger}(\mathbf{k}', \omega')] = \delta_{\sigma\sigma'} \delta(\mathbf{k} - \mathbf{k}') \delta(\omega - \omega'). \quad (49)$$

The quantum optical effective-index theory for planar metamaterials is hereby defined. Based on these expressions for the effective output operators and their commutators, we will in Sec. V compare predictions for physical observables using the quantum optical effective-index theory as compared to the full multilayer quantum theory of the previous section.

V. FIRST TEST: POWER SPECTRA

As a first test and comparison of the quantum optical effective-index theory, we will now study the output intensities of light due to spontaneously emitted photons. If atoms that make up the metamaterial are excited, either thermally or because of external pumping, then they can decay spontaneously. This is a known noise source in lasers, which is typically overlooked for metamaterials. There is a variety of different quantum definitions of the power spectrum in the literature [64]. Here we choose the quantum generalization of the classical definition of the energy spectrum for the case of a stationary field [64]. Just like its classical counterpart, it is directly related to observables in light detection experiments. For sufficiently small pass-band width of the spectral apparatus, the power spectrum $\mathcal{S}(\mathbf{x}, \omega)$ of the light emitted on the right-hand side of our multilayer metamaterial of Fig. 1 is given by

$$\mathcal{S}(\mathbf{x}, \omega) = \lim_{T \rightarrow \infty} \frac{1}{2\pi T} \iint_{-T/2}^{T/2} dt dt' e^{-i\omega(t-t')} \langle \mathbf{E}^{(N+1)-}(\mathbf{x}, t) \cdot \mathbf{E}^{(N+1)+}(\mathbf{x}, t') \rangle, \quad (50)$$

where ω is the operating frequency of the spectral apparatus, and T is the duration the detector is switched on. Here, the positive-frequency part of the electric field operator $\mathbf{E}^{N+1(+)}$ can now be determined with the help of Eq. (27). As usual the negative-frequency part of the field is obtained by taking the Hermitian conjugate of

Eq. (28). We will also need the input-output relation (38) to express the annihilation and creation operators of the outgoing field on the right-hand side of the multilayer in terms of the operators of the ingoing fields and of the quantum noise. The power spectrum (50) can then be written as

$$\begin{aligned} \mathcal{S}(z, \omega) = & \frac{\hbar\omega^2}{2\varepsilon_0 c^2} \sum_{\sigma} \int d\mathbf{k} \beta_0^{-1} \left\{ \langle a_{\sigma,-}^{(N+1)\dagger}(z, \mathbf{k}, \omega) a_{\sigma,-}^{(N+1)}(z, \mathbf{k}, \omega) \rangle \left(|\mathcal{A}_{\sigma,22}|^2 + e^{-2i\beta_0 z} \mathcal{A}_{\sigma,22}^* \varrho_{\sigma,-}^{(N+1)} \right. \right. \\ & \left. \left. + e^{2i\beta_0 z} \mathcal{A}_{\sigma,22} \varrho_{\sigma,-}^{(N+1)} + 1 \right) \right. \\ & + \langle a_{\sigma,-}^{(N+1)\dagger}(z, \mathbf{k}, \omega) a_{\sigma,+}^{(1)}(z, \mathbf{k}, \omega) \rangle \left(\mathcal{A}_{\sigma,21} \mathcal{A}_{\sigma,22}^* + e^{2i\beta_0 z} \mathcal{A}_{\sigma,21} \varrho_{\sigma,-}^{(N+1)} \right) \\ & + \langle a_{\sigma,+}^{(1)\dagger}(z, \mathbf{k}, \omega) a_{\sigma,-}^{(N+1)}(z, \mathbf{k}, \omega) \rangle \left(\mathcal{A}_{\sigma,21}^* \mathcal{A}_{\sigma,22} + e^{-2i\beta_0 z} \mathcal{A}_{\sigma,21}^* \varrho_{\sigma,-}^{(N+1)} \right) \\ & \left. + \langle a_{\sigma,+}^{(1)\dagger}(z, \mathbf{k}, \omega) a_{\sigma,+}^{(1)}(z, \mathbf{k}, \omega) \rangle |\mathcal{A}_{\sigma,21}|^2 \right\} + \mathcal{S}_{\text{Spon}}(\omega), \quad (51) \end{aligned}$$

where the parameters $\varrho_{\sigma,-}^{(N+1)}$ equal to unity and $(2k^2 c^2 / \omega^2 - 1)$ for s - and p -polarized light, respectively, so they coincide for normal incidence as they should. Expectation values are denoted by brackets. Thanks to the input-output theory, the brackets occur around products of input operators and all expectation values are taken with respect to both the states of the incoming optical fields and the states of the noise fields within all medium layers. All terms except the last one on the right-hand

side of Eq. (51) describe output photons caused by (multiple) reflections and transmissions of input photons. The final term $\mathcal{S}_{\text{Spon}}(\mathbf{x}, \omega)$ on the other hand is independent of the optical input signal, and is determined by the quantum noise in the medium, especially by the properties of the noise operators defined in Eq. (39), as detailed below. Physically, thermal excitations in passive layers and especially pumped excitations in amplifying layers give rise to spontaneously emitted noise photons.

We want to know how well quantum optical effective-medium theories describe the amount of quantum noise photons that contribute to photon-counting measurements. In this section we will therefore study output intensities in the absence of any optical input signal, in other words all optical incoming fields are assumed to be in the vacuum state $|0\rangle$. In that simple case all terms except the last one in Eq. (51) vanish identically and all output photons are spontaneously emitted noise photons, or $\mathcal{S}(\mathbf{x}, \omega) = \mathcal{S}_{\text{Spon}}(\mathbf{x}, \omega)$. We will now use our input-output formalism once more, this time to express the spontaneously emitted light in terms of the noise sources in the multilayer medium. In particular, using the matrix form (40b) of the factors $\mathcal{B}^{(j)}$, the power spectrum (51)

becomes

$$\begin{aligned} \mathcal{S}_{\text{Spon}}(\omega) &= \sum_{\sigma} \int_0^{\pi/2} d\theta \mathcal{S}_{\text{Spon},\sigma}(\theta, \omega) \\ &= \frac{\hbar\omega^2}{8\pi^2\varepsilon_0c^2} \sum_{\sigma} \int d\mathbf{k} \beta_0^{-1} \langle F_{\sigma,+}^{\dagger}(\mathbf{k}, \omega) F_{\sigma,+}(\mathbf{k}, \omega) \rangle \end{aligned} \quad (52)$$

from which it is clear that indeed the power spectrum of the spontaneously emitted light depends on the quantum noise through the expectation value of $\langle F_{\sigma,+}^{\dagger}(\mathbf{k}, \omega) F_{\sigma,+}(\mathbf{k}, \omega) \rangle$. Exact multilayer theory, in particular Eqs. (34) and (39), then gives the following exact long expression for the flux of noise photons emitted from the loss-compensated multilayer

$$\begin{aligned} \langle F_{\sigma,+}^{\dagger}(\mathbf{k}, \omega) F_{\sigma',+}(\mathbf{k}', \omega') \rangle_{\text{exact}} &= 2 \sum_{j=2}^N \left\{ \rho_{\sigma,+}^{(j)} \sinh(\beta_j'' l_j) \text{sgn}[\varepsilon_{1j}(\omega)] \left(|\mathcal{B}_{\sigma 21}^{(j)}|^2 e^{-\beta_j'' l_j} + |\mathcal{B}_{\sigma 22}^{(j)}|^2 e^{\beta_j'' l_j} \right) \right. \\ &\quad \left. - \frac{|\beta_j''|}{\beta_j'} \rho_{\sigma,-}^{(j)} \sin(\beta_j' l_j) \left(\mathcal{B}_{\sigma 21}^{(j)*} \mathcal{B}_{\sigma 22}^{(j)} e^{i\beta_j'(z_j+z_{j-1})} + \mathcal{B}_{\sigma 21}^{(j)} \mathcal{B}_{\sigma 22}^{(j)*} e^{-i\beta_j'(z_j+z_{j-1})} \right) \right\} \\ &\times (N_{\text{th}}(\omega, T) \Theta[\varepsilon_{1j}(\omega)] + (N_{\text{th}}(\omega, |T|) + 1) \Theta[-\varepsilon_{1j}(\omega)]) \delta_{\sigma\sigma'} \delta(\omega - \omega') \delta(\mathbf{k} - \mathbf{k}'). \end{aligned} \quad (53)$$

While this formula is valid for all temperatures, in the following we will mostly consider power spectra at zero temperature. Passive media do not emit thermal photons in that case, but amplifying layers have population inversion and their excited-state population can decay spontaneously. In our numerical examples, we will look at the polarization-and angle-dependent

power spectrum $\mathcal{S}_{\text{Spon},\sigma}(\theta, \omega)$ that was defined in terms of $\langle F_{\sigma,+}^{\dagger}(\mathbf{k}, \omega) F_{\sigma',+}(\mathbf{k}', \omega') \rangle$ in the second equality of Eq. (52), and where we assumed that only propagating modes reach the detector and thus restricted the Fourier integral to modes with $|\mathbf{k}| > \omega/c$. For definiteness, for loss-compensated metamaterials at zero temperature the angle-dependent power spectrum is given by

$$\begin{aligned} \mathcal{S}_{\text{Spon},\sigma}(\theta, \omega) &= \frac{-\hbar\omega^3 \sin\theta}{2\pi\varepsilon_0c^3} \sum_{j=1}^{\frac{N}{2}-1} \left\{ \varrho_{\sigma,+}^{(2j+1)} \sinh(\beta_{2j+1}'' d_g) \left(|\mathcal{B}_{\sigma 21}^{(2j+1)}|^2 e^{-\beta_{2j+1}'' d_g} + |\mathcal{B}_{\sigma 22}^{(2j+1)}|^2 e^{\beta_{2j+1}'' d_g} \right) \right. \\ &\quad \left. + \varrho_{\sigma,-}^{(2j+1)} \frac{|\beta_{2j+1}''|}{\beta_{2j+1}'} \sin(\beta_{2j+1}' d_g) \left(\mathcal{B}_{\sigma 21}^{(2j+1)*} \mathcal{B}_{\sigma 22}^{(2j+1)} e^{i\beta_{2j+1}'(z_{2j+1}+z_{2j})} \right. \right. \\ &\quad \left. \left. + \mathcal{B}_{\sigma 21}^{(2j+1)} \mathcal{B}_{\sigma 22}^{(2j+1)*} e^{-i\beta_{2j+1}'(z_{2j+1}+z_{2j})} \right) \right\}. \end{aligned} \quad (54)$$

This formula predicts the output intensity of light by summing up all processes by which photons are spontaneously generated in the amplifying layers and, after reflections and transmissions, with some probability end up in the output channel of our interest.

What corresponding power spectrum does the quantum optical effective-index theory of Sec. IV predict? From the definitions (46) together with the commutation relation (47), the flux of noise photons emitted by the multilayer slab at a finite temperature T can within the effective-index theory be expressed in terms of the

effective reflection and transmission amplitudes as

$$\begin{aligned} \langle F_{\text{eff},\sigma,\pm}^{\dagger}(\mathbf{k}, \omega) F_{\text{eff},\sigma',\pm}(\mathbf{k}', \omega') \rangle_{\text{QOEI}} &= \\ &\{ N_{\text{th}}(\omega, T) \Theta[\varepsilon_{\text{Ieff}}(\omega)] - (N_{\text{th}}(\omega, |T|) + 1) \Theta[-\varepsilon_{\text{Ieff}}(\omega)] \} \\ &\times (1 - |r_{\text{eff},\sigma}|^2 - |t_{\text{eff},\sigma}|^2) \delta_{\sigma\sigma'} \delta(\mathbf{k} - \mathbf{k}') \delta(\omega - \omega'). \end{aligned} \quad (55)$$

Here k_B is the Boltzmann constant and T is temperature, and $N_{\text{th}} = 1/(\exp[\hbar\omega/k_B T] - 1)$ is the thermal distribution of photon states at energy $\hbar\omega$. Notice that this flux of noise photons in Eq. (55) is always a non-negative quantity (as it should be): for media that are effectively

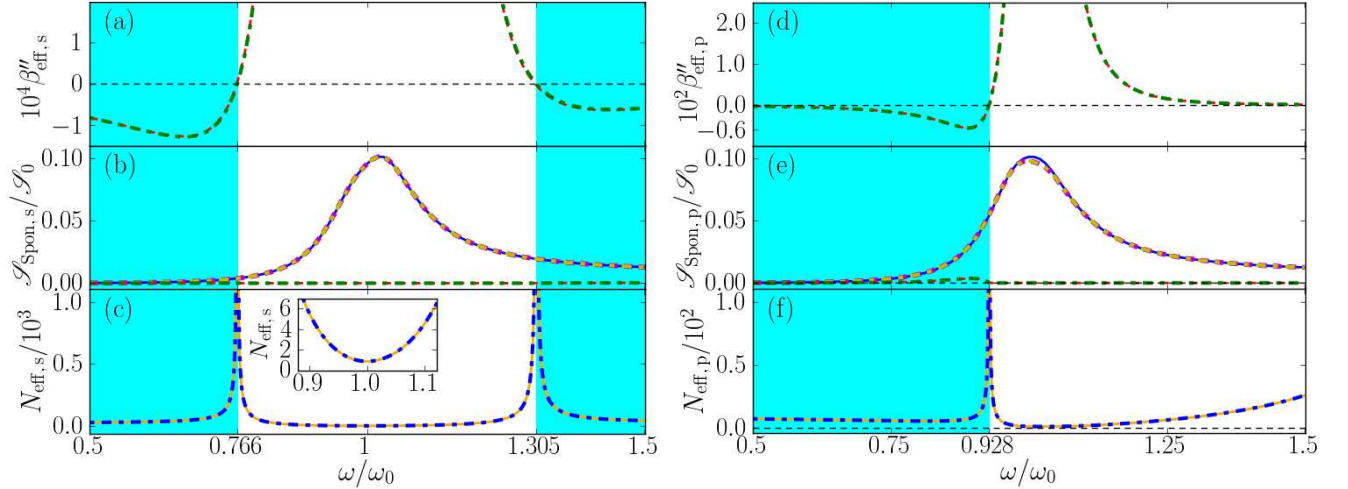


FIG. 2. Power spectrum (54) of spontaneous emission of noise photons exiting a loss-compensated multilayer metamaterial at an angle of 30 degrees away from the normal, in units of $\mathcal{S}_0 = \hbar\omega_0^3/4\pi\epsilon_0c^3$, due to spontaneous emission of noise photons within the loss-compensated multilayer metamaterial of Fig. 6, at zero temperature. Left and right panels correspond to s - and p -polarized light, respectively. The amplifying and absorbing layers are described by the Lorentz model [Eq. (56)], with parameters $\omega_{pa}/\omega_0 = 0.3$, $\gamma_a/\omega_0 = 0.1$ for the lossy layers, and $\omega_{pb}/\omega_0 = 0.25$, $\gamma_b/\omega_0 = 0.15$ for the layers with gain. We choose $d_{a,b}\omega_0/c = 0.1$ and five unit cells. The parts (a) and (d) show the imaginary part of the normal wave-vector component β_{eff} . In panels (b) and (e), the power spectrum of the noise photons predicted with the effective-index theories is compared to the exact multilayer calculation and the QOEM theory. For the effective-index theories, red dotted curves are obtained by inserting effective parameters based on Eq. (A1) into Eq. (54); the green dash-dotted lines correspond to the other procedure Eq. (A3) to obtain effective parameters. Similarly, for QOEM theory (discussed in Sec. VI) the magenta dashed lines are produced with Eq. (A1), and the yellow dash-dotted curves with Eq. (A3). Panels (c) and (f) show the effective noise current densities N_{eff} of Eq. (59), in solid orange lines as obtained using the effective index of Eq. (A1) and in dash-dotted blue curves as produced with the other procedure [Eq. (A3)] to obtain the effective index.

absorbing at frequency ω , the $\epsilon_{\text{Ieff}}(\omega)$ is positive and so is $(1 - |r_{\text{eff},\sigma}|^2 - |t_{\text{eff},\sigma}|^2)$, while for effectively amplifying media, both these quantities are negative. The form of the power spectrum of the spontaneously emitted light (52) within the effective-index theory is now obtained by substituting Eqs. (55) and (45) into Eq. (52).

To be specific, unless stated explicitly, below in our numerical examples we will assume the temperature to be zero Kelvin. Furthermore, we will assume that lossy and amplifying layers can be described by Lorentzian dielectric functions. A medium consisting of two-level atoms with a population N_{up} in the upper level and N_{down} in the lower level can near its resonance frequency ω_0 be described by an electric permittivity of the Lorentzian form [55]

$$\epsilon(\omega) = 1 + \left(\frac{N_{\text{down}} - N_{\text{up}}}{N_{\text{down}} + N_{\text{up}}} \right) \frac{\omega_p^2}{\omega_0^2 - \omega^2 - i\gamma\omega}. \quad (56)$$

where ω_p is the coupling frequency, ω_0 is the transverse resonance frequency, and γ is the dissipation and amplification parameters for lossy and amplifying layers, respectively. The population factor that occurs in the dielectric function (56) is positive for passive systems, $N_{\text{down}} > N_{\text{up}}$, but negative for optical gain that arises from population inversion in the medium, $N_{\text{up}} > N_{\text{down}}$. In addition, this factor can be written in term of the

thermal distribution N_{th} as $(2N_{\text{th}}(\omega, T) + 1)^{-1}$ for lossy and as $(-2N_{\text{th}}(\omega, |T|) - 1)^{-1}$ for amplifying layers. In Figure 2 we explore regions with net loss and net gain and the frequencies of exact loss compensation that separate them, and study the corresponding flux of noise photons and the effective noise photon distribution, all corresponding to an output angle of 30°. Left panels depict s - and right panels p -polarization. In Figure 3

we show the analogous results for an emission angle of 60°. (Some panels of the two figures will be explained below in Sec. VI.)

Exact loss compensation occurs when the imaginary part of the normal-wave vector components β_{eff} vanishes. We show β_{eff} in panels (a) and (d) of both figures, where it is also clear that the two methods to retrieve effective parameters lead to nearly identical results. For s -polarization, it follows from Eq. (A3) that exact loss compensation occurs at angle-independent frequencies. A comparison of the panels (a) of Figs. 2 and 3 illustrates this, where for the parameters chosen, exact loss compensation occurs at angle-independent frequencies. A net loss in the frequency range $0.766358 < \omega/\omega_0 < 1.30487$ and net gain at elsewhere.

By contrast, for p -polarized light exact loss compensation does depend on the angle of incidence, as again follows from Eq. (A3) and as illustrated in Figs. 2 and 3: in Fig. 2(d) exact loss compensation occurs (only) at

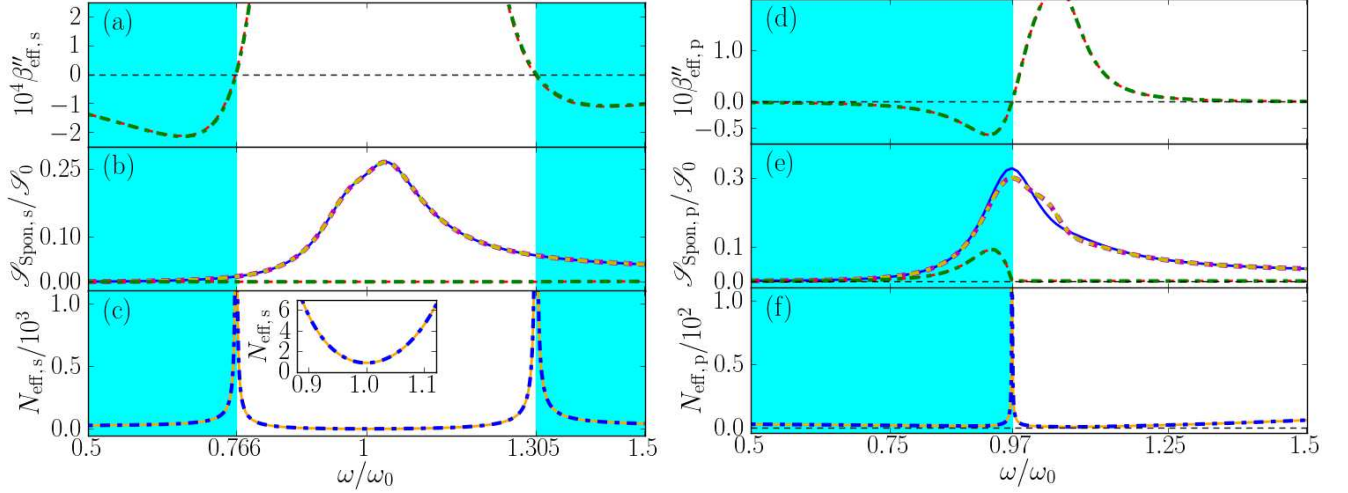


FIG. 3. As in Fig. (2) but now for light emission at an angle of 60 degrees with respect to the normal.

$\omega = 0.928424\omega_0$, with net gain at smaller and net loss at higher frequencies. At sixty degrees, Fig. 3(d) shows exact loss compensation at a slightly higher frequency.

In panels (b) for s -polarization and (e) for p -polarization, power spectra are displayed for spontaneously emitted light that exits the metamaterial at an angle of 30° (Fig. 2) and 60° (Fig. 3). Note that these angular power spectra are continuous also across frequencies of exact loss compensation.

It is known that for lossy homogeneous media at zero temperature the flux of noise photons vanishes, so the power spectrum of the outgoing noise photons vanishes. The effective-index theory predicts something else, namely that no photons are emitted by *effectively* lossy loss-compensated metamaterials. This prediction is illustrated in panels (b) and (e) of Figs. 2 and 3, especially around ω_0 for outgoing s -polarized light, and above $0.928424\omega_0$ for outgoing p -polarized light. By contrast, the full gain-loss multilayer calculation does predict the emission of noise photons at zero temperature, as the figures show. Thus effective-index theory clearly fails for effectively lossy loss-compensated metamaterials. At exact loss compensation ($\varepsilon_{\text{Ieff}} = 0$), by Eq. (55) the effective-index theory predicts that the flux of noise photons vanishes, which the figures show is another failure of the effective-index theory.

For effectively amplifying loss-compensated metamaterials, the effective-index theory does predict a finite flux of spontaneously emitted photons that grows with the effective gain, as is best visible in Fig. 3(d), where for frequencies slightly below $0.97\omega_0$ much loss is slightly

overcompensated by much gain. Again the effective-index theory is clearly far from accurate. Hence, for loss-compensated metamaterials at zero temperature, we find a clear failure of the quantum optical effective-index theory to predict an accurate power spectrum for loss-compensated metamaterials. A new effective theory is needed that also accurately describes the amount of noise photons in metamaterials.

VI. QUANTUM OPTICAL EFFECTIVE-MEDIUM THEORY

We will now derive a quantum-optical effective medium (QOEM) theory that does give accurate predictions for three-dimensional light propagation in loss-compensated media. In contrast to the previous effective theory, it is not an effective-index theory, because besides the effective index another effective parameter will be needed. Our approach is to distill solely from a unit cell not only the usual $\beta_{\text{eff},\sigma}$ but also an effective noise photon distribution $N_{\text{eff},\sigma}(\mathbf{k}, \omega, T)$. The theory presented here is a generalization of Ref. 45, which is valid for normal incidence, to arbitrary angles of incidence.

Analogous to effective-index theory, we will again assume that there is an effective noise operator in the unit cell. However, unlike in the effective-index theory we will not try not define this operator, but rather determine the expectation value of its corresponding number operator. Analogous to Eq. (55) for the effective-index theory, we will write the expectation value

$$\begin{aligned} \langle F_\sigma^\dagger(\mathbf{k}, \omega) F_{\sigma'}(\mathbf{k}', \omega') \rangle_{\text{QOEM}} &= \{ N_{\text{eff},\sigma}(\mathbf{k}, \omega, T) \Theta[\varepsilon_{\text{unit,eff I}}(\omega)] - (N_{\text{eff},\sigma}(\mathbf{k}, \omega, |T|) + 1) \Theta[-\varepsilon_{\text{unit,eff I}}(\omega)] \} \\ &\times (1 - |R_{\text{unit,eff},\sigma}|^2 - |T_{\text{unit,eff},\sigma}|^2) \delta_{\sigma\sigma'} \delta(\mathbf{k} - \mathbf{k}') \delta(\omega - \omega'), \end{aligned} \quad (57)$$

in terms of the effective noise current density N_{eff} that we

define shortly. The $R_{\text{unit,eff},\sigma}$ and $T_{\text{unit,eff},\sigma}$ are the (clas-

sical) reflection and transmission amplitudes of the entire unit cell. If the factor $(1 - |R_{\text{unit,eff},\sigma}|^2 - |T_{\text{unit,eff},\sigma}|^2)$ is positive then it quantifies the amount of net absorption in the unit cell, otherwise it quantifies the net amount of amplification. The difference with Eq. (55) for the effective-index theory that featured thermal distributions N_{th} is thus that here instead we defined an effective distribution that in general is not a thermal one.

We fix $\langle F^\dagger F \rangle_{\text{QOEM}}$ of Eq. (57) and thereby N_{eff} in three steps. First, we apply our general input-output theory of Sec. III to a single unit cell of the metamaterial. Second, we require that the expectation value $\langle F^\dagger F \rangle_{\text{QOEM}}$ coincides with the corresponding unit-cell-averaged noise expectation value of the general multilayer theory. Third, we make use of our assumption that the unit cell of the metamaterial is much thinner than an optical wavelength, so we can Taylor expand the results from multilayer theory to first order in the layer thicknesses $d_{a,b}$ and obtain

$$\langle F_\sigma^\dagger(\mathbf{k}, \omega) F_{\sigma'}(\mathbf{k}', \omega') \rangle_{\text{QOEM}} = \sum_{j=a,b} \frac{d_j |\varepsilon_{j,I}| \omega^2 \mathcal{K}_{j,\sigma}(\theta)}{c^2 \beta_0} \times N_{\text{th}}(\omega, |T_j|) \delta_{\sigma\sigma'} \delta(\mathbf{k} - \mathbf{k}') \delta(\omega - \omega'), \quad (58)$$

where $\mathcal{K}_{j,s}(\theta) = 1$ and $\mathcal{K}_{j,p}(\theta) = (\sin^2 \theta + |\varepsilon_j|^2 \cos^2 \theta) / |\varepsilon_j|^2$. Now we have two expressions for $\langle F^\dagger F \rangle_{\text{QOEM}}$, namely Eqs. (57) and (58). By equating these two, Taylor approximating also the net gain or loss factor $(1 - |R_{\text{unit,eff},\sigma}|^2 - |T_{\text{unit,eff},\sigma}|^2)$ of Eq. (57) to first order in the unit cell thickness $d = d_a + d_b$, and solving for $N_{\text{eff},\sigma}(\mathbf{k}, \omega)$, we obtain as a main result this effective noise photon distribution

$$N_{\text{eff},\sigma} = \begin{cases} \sum_{j=a,b} \eta_{j,\sigma} [N_{\text{th}}(\omega, T_j)] \\ -1 + \sum_{j=a,b} \eta_{j,\sigma} [N_{\text{th}}(\omega, |T_j|) + 1] \\ -\frac{1}{2} + \frac{1}{2} \sum_{j=1,g} \eta_{j,\sigma} [2N_{\text{th}}(\omega, |T_j|) + 1] \end{cases} \quad (59)$$

which correspond, from top to bottom, to loss-loss, gain-gain, and loss-compensated metamaterials. This effective noise photon density thus depends on the same variables as the classical effective parameter β_{eff} : on the angle of incidence, on the polarization of the input state, as well as on the dielectric parameters of the unit cell via

$$\eta_{j,\sigma}(\theta) = p_j \frac{\mathcal{K}_{j,\sigma}(\theta)}{\mathcal{K}_{\text{eff},\sigma}(\theta)} \left| \frac{\varepsilon_{j,I}(\omega)}{\varepsilon_{\text{eff},I}(\omega)} \right|, \quad (60)$$

where the $p_j = d_j/d$ are the volume fractions of the layers and $\mathcal{K}_{\text{eff},\sigma}(\theta)$ equals $\mathcal{K}_{j,\sigma}(\theta)$ with ε_j replaced by ε_{eff} . We allowed the two types of layers of the unit cell to be at different temperatures. Generalizations to more than two layers are straightforward.

Let us first apply this QOEM theory to loss-compensated metamaterials. In panels (b) and (e) of Figs. 2 and 3 we showed power spectra, and found that the exact multilayer theory predicts quite a lot more noise photons than the effective-index theory did. By contrast, the curves of QOEM theory almost coincide with the exact multilayer result in all these panels. This

illustrates that we have an accurate quantum optical effective-medium theory for three-dimensional light propagation in multilayer metamaterials, both for *s*- and *p*-polarized light.

What do we know about the new effective parameter, the effective noise photon distribution? To gain some intuition, notice that from Eqs. (59) and (60) it follows that N_{eff} grows when loss in the metamaterial is more exactly compensated by gain [smaller $\varepsilon_{\text{eff},I}(\omega)$] or when the same value $\varepsilon_{\text{eff},I}(\omega)$ results from compensating more loss by more gain (i.e. with $|\varepsilon_{a,I}(\omega)|$ and $|\varepsilon_{b,I}(\omega)|$ both larger). This is illustrated in panels (c) and (f) of Figs. 2 and 3, where we see that N_{eff} even diverges at exact loss compensation, but in such a way as to keep the power spectra at those frequencies continuous. This means that for metamaterials with more effective loss compensation, it becomes increasingly important to use N_{eff} as an additional effective-medium parameter instead of N_{th} . These results illustrate that we have successfully generalized the one-dimensional QOEM theory of our Ref. 45 to light propagation in three dimensions.

Let us now show that our new QOEM theory indeed reduces to the one of Ref. 45 in case of light propagation perpendicular to the interface, i.e. for $\mathbf{k} = \mathbf{0}$. In that case, the parameter $\mathcal{K}_{j,\sigma}(\theta)$ in Eq. (58) tends to unity for both polarizations. This in turn implies that the parameter $\eta_{j,\sigma}(\theta)$ defined in Eq. (60) tends to $p_j |\varepsilon_{j,I}(\omega)| / \varepsilon_{\text{eff},I}(\omega)$. This indeed agrees with Ref. 45, where we showed that the quantum optical effective-medium theory with N_{eff} for normal incidence gave accurate predictions for loss-compensated, loss-loss as well as gain-gain metamaterials.

Do we also need the QOEM theory for loss-loss or gain-gain metamaterials? If the two layers within the unit cell are somehow kept at different temperatures, then we do, but this is not easy to realize. But if the entire unit cell is kept at the same temperature, then for light propagation normal to the layers we found in Ref. 45 that QOEM theory reduces to the quantum optical effective-index theory, i.e. N_{eff} becomes equal to the thermal noise photon distribution N_{th} . Is this also true in three dimensions? Let us consider *s*-polarized light first, for loss-loss and gain-gain metamaterials at a uniform temperature ($T_a = T_b$). This means technically that the thermal distributions in Eq. (59) can be moved in front of the summation, and the remaining summation is $\sum_{j=a,b} \eta_{j,s}(\theta)$. Since in $\eta_{j,s}(\theta)$ as defined in Eq. (60) the fractions $\mathcal{K}_{j,s}(\theta) / \mathcal{K}_{\text{eff},s}(\theta)$ are equal to unity, the sum $\sum_{j=a,b} \eta_{j,s}(\theta)$ becomes $\sum_{j=a,b} p_j |\varepsilon_{j,I}(\omega)| / \varepsilon_{\text{eff},I}(\omega)$, which is angle independent. In Ref. 45 we also pointed out that for normal incidence the sum $\sum_{j=a,b} p_j |\varepsilon_{j,I}(\omega)| / \varepsilon_{\text{eff},I}(\omega)$ adds up to unity for loss-loss and gain-gain metamaterials (whereas the sum is always larger than unity for loss-compensated (gain-loss) metamaterials). So now we find that for *s*-polarized light, the same relations even hold for arbitrary angles of incidence, as illustrated by the horizontal line in Figure 4(a). This angle-independence for *s*-polarized light is related to the fact that for arbitrary propagation direc-

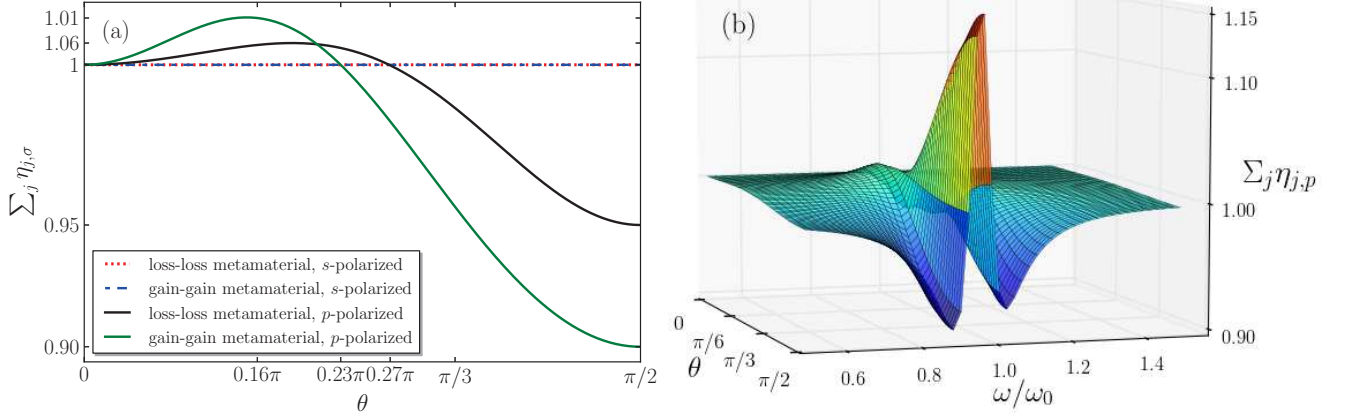


FIG. 4. (Color online) (a) The sum $\sum_{j=a,b} \eta_{j,\sigma}$ is shown as a function of the angle of incidence θ for s -polarized component of input light impinging on the loss-loss (dotted red line) and the gain-gain (dash-dotted blue line) multilayers, and p -polarized component of input light incident on the loss-loss (solid black line) and the gain-gain (solid green line) multilayers. (b) The sum $\sum_{j=a,b} \eta_{j,p}$ is shown as a function of the angle of incidence θ and of the dimensionless frequency ω/ω_0 for p -polarized component of input light impinging on a gain-gain multilayer. The multilayer metamaterial with geometry of Fig. 6 has alternating layers with equal thickness $d_{a,b}\omega_0/c = 0.1$, with dielectric parameters in Eq. (56): $\omega_{p_a}/\omega_0 = 0.3$, $\omega_{p_b}/\omega_0 = 0.1$ and $\gamma_{a,b}/\omega_0 = 0.1$. In panel (a), we choose $\omega/\omega_0 = 0.9$.

tions the electric-field components are parallel to the interface, just like for normal incidence. As a consequence, we find that for s -polarized light, the effective noise photon distribution $N_{\text{eff},s}$ reduces to the thermal distribution N_{th} . So both for a lossy metamaterial at a homogeneous positive temperature and for an amplifying metamaterial at a spatially constant negative temperature, the QOEM theory for s -polarized light reduces to the quantum optical effective-index theory.

How about p -polarized light then, does N_{eff} also reduce to the thermal distribution for loss-loss and gain-gain metamaterials? For MMs kept at a uniform temperature, the thermal factor in the summation of Eq. (59) can again be put in front, so that the summation reduces to $\sum_{j=a,b} \eta_{j,p}(\theta)$. However, for p -polarized light the fractions $\mathcal{K}_{j,p}(\theta)/\mathcal{K}_{\text{eff},p}(\theta)$ do not give unity, and hence the sum $\sum_{j=a,b} \eta_{j,p}(\theta)$ in general does not add up to unity. The angle dependence of this sum is illustrated in Fig. 4(a). For small angles, the sum is larger than unity while for large angles it is smaller than unity.

As a consequence, for p -polarized light N_{eff} in general does not reduce to the thermal distribution, and consequently the QOEM theory does not reduce to the quantum optical effective-index theory. For the parameters as in Fig. 4, N_{eff} becomes larger (smaller) than the thermal distribution N_{th} for angles of incidence smaller (larger) than 0.27π for the loss-loss metamaterial, and for the gain-gain MM the critical angle occurs at 0.23π . This difference between the effective and thermal distributions also in metamaterials without loss compensation is a qualitatively new finding as compared to the previous results of Ref. 45 for one-dimensional light propagation.

Quantitatively, the deviations of N_{eff} from a thermal distribution are relatively small, within ten percent for

the specific dielectric parameters chosen in Fig. 4(a). The closer the sum $\sum_j \eta_{j,p}$ comes to unity, the closer QOEM theory comes to the quantum optical effective-index theory becomes. This sum is thus a measure for the “distance” between the two theories, and it depends on the dielectric parameters of the unit cell. Moreover, it depends on the angle of incidence and on the frequency of light how much the two theories will agree for p -polarization. In order to illustrate both dependencies, in Fig. 4(b) we depict the sum $\sum_j \eta_{j,p}$ as a function of both the angle of incidence θ and of the dimensionless frequency ω/ω_0 , for the same gain-gain MM as in Fig. 4(a). For all combinations of parameters considered in Fig. 4(b), we find that the sum has a maximal deviation from unity of around 15 percent. We find similar modest but non-negligible frequency and angle dependence (not shown) for the loss-loss multilayer of Fig. 4(a).

In Figure 5 we compare power spectra for p -polarized light exiting at an angle of 60 degrees away from the normal of the MM, computed with the exact multilayer theory, with QOEM theory, and with the quantum optical effective-index theory. The left panels are for loss-loss MMs, the right panels for gain-gain MMs, upper panels for zero temperature and lower panels for elevated temperature. In panel (a) for the loss-loss multilayer at zero temperature, quantum noise can be neglected, so just like in classical optics the power spectrum of output light vanishes identically and perfect agreement between all curves is observed. By contrast, for the gain-gain multilayer at zero temperature in panel 5(b), the population of the two-level medium is fully inverted and the effects of quantum noise in the output cannot be neglected. The power spectrum of output light appears as a peak near ω_0 which is associated with the resonance frequency of the

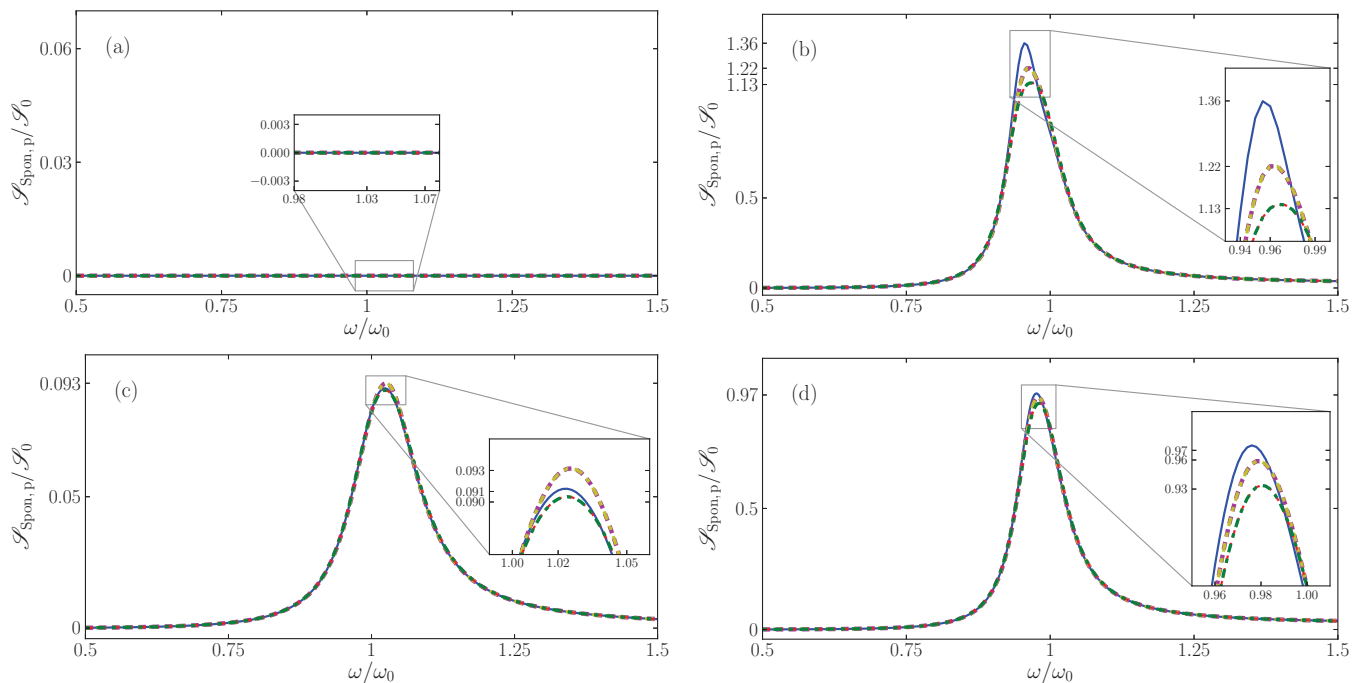


FIG. 5. The spontaneous-emission power spectrum of the noise photons (54), in units of $\mathcal{S}_0 = \hbar\omega_0^3/4\pi\epsilon_0c^3$, for p - polarized light exiting the MM at 60 degrees away from the normal direction. In all four panels, the QOEM theory and the quantum optical effective-index theory are compared to the exact multilayer calculation. For the exact multilayer calculation (solid blue curves), the loss and gain layers are described by Lorentz model with parameters are identical to those used in Fig. 4. Left and right panels correspond to loss-loss and gain-gain metamaterials with the geometry of Fig. 6. The loss-loss and the gain-gain multilayer are maintained at zero temperature in panels (a) and (b), and at the elevated positive temperature $T = 0.6\hbar\omega_0/k_B$ in panel (c), and at the elevated negative temperature $|T| = 0.6\hbar\omega_0/k_B$ in (d). For the effective-index theories, red dotted and green dash-dotted curves present the numerical parameters as obtained from the scattering method (A1) and the dispersion method (A3), respectively. For QOEM theory, magenta dashed and yellow dash-dotted lines correspond to these same classical effective parameter retrieval methods (A1) and (A3). These effective parameters so obtained are also used to compute N_{eff} .

dielectric functions of each layer. Away from resonance, both effective theories agree with the exact calculation. Near resonance there are small differences on the order of a few percent between the exact multilayer calculation and the two effective-medium theories. As seen in the zoomed inset in Fig. 5(b), near the resonance the QOEM theory is slightly more accurate than the effective-index theories.

In panels 5(c) for loss-loss MMs at a pretty high temperature and 5(d) for gain-gain MMs at a negative temperature, the exact and the two effective power spectra again agree quite well, with only on resonance a few percent difference. Sufficiently far from the resonance when absorption is small, the thermal noise becomes negligibly small and the power spectrum of output noise photons is approximately zero. For the gain-gain multilayer the amplitude of the peak in panel (d) is smaller than the one in (b) since amplification within gain layers is reduced by saturation effects. We checked (but do not show it here) that these results do not depend much on the typical parameters used in Fig. 5. The overall message of Fig. 5 is that both the QOEM theory and the quantum optical effective-index theory are quite accurate in describing power spectra of p -polarized light of loss-loss and

gain-gain metamaterials, with the two effective theories almost equally accurate. So one can use either N_{eff} or N_{th} as the noise photon distribution in Eq. (55).

To summarize our findings from this section, we compared for the first time power spectra of metamaterials based on exact theory and on QOEM and effective-index theory. For loss-compensated metamaterials we find that the effective-index theory is manifestly inadequate, both for s - and p -polarized light. By contrast, our QOEM theory in a consistent way predicts that the quantum noise contribution $\langle F_\sigma^\dagger(\mathbf{k}, \omega) F_{\sigma'}(\mathbf{k}', \omega') \rangle$ to the power spectrum of a layered metamaterial is given by Eq. (55), but with the thermal distribution $N_{\text{th}}(\omega, |T|)$ replaced by the effective distribution $N_{\text{eff}, \sigma}(\mathbf{k}, \omega, T)$ of Eq. (59). In the absence of loss compensation, i.e. for loss-loss and gain-gain metamaterials, we found that for s -polarized light the QOEM theory exactly coincides with the quantum optical effective-index theory. For p -polarization there is no such exact agreement in the absence of loss compensation, but numerically the differences between both effective theories are so small that it is essentially a matter of choice which one to use. For loss-compensated metamaterials, QOEM theory is the only accurate effective-medium theory.

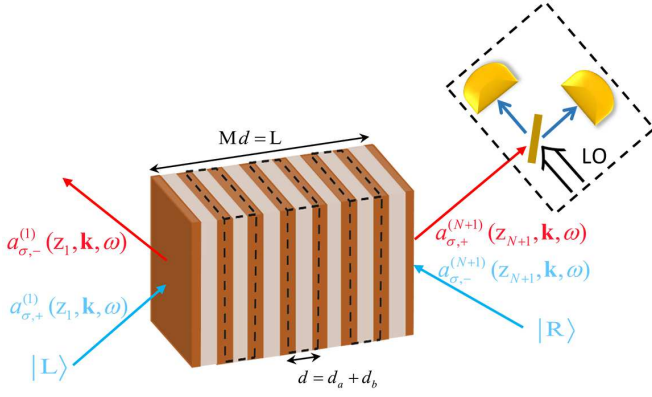


FIG. 6. (Color online) Scheme of the loss-compensated multilayer medium in air. It has alternating layers with thicknesses $d_{a,b}$ that are arranged symmetrically. The two outermost layers have widths $d_a/2$, which makes the medium finite periodic with M unit cells. The amplifying and absorbing layers are described by the Lorentz model [Eq. (56)], with parameters $\omega_{pa}/\omega_0 = 0.3$, $\gamma_a/\omega_0 = 0.1$ for the lossy layers, and $\omega_{pb}/\omega_0 = 0.25$, $\gamma_b/\omega_0 = 0.15$ for the layers with gain. We choose $d_{a,b}\omega_0/c = 0.1$ and $M = 5$. The incident squeezed vacuum state $|L\rangle$ has the squeeze strength $\zeta_\sigma = 0.2$ and phase $\phi_{\sigma,\zeta} = 2\phi_{\sigma,LO} - \frac{\pi}{2}$, while the squeezed vacuum state $|R\rangle$ has the same strength $\xi_\sigma = 0.2$ with $\phi_{\sigma,\xi} = 2\phi_{\sigma,LO} - 2$, all assumed to be frequency independent. The outgoing light on the right-hand side of the multilayer metamaterial is measured with a balanced homodyne detector, shown within the dashed box, which is assumed to co-rotate with the angle θ .

VII. SECOND TEST: PROPAGATION OF SQUEEZED STATES

For the power spectra emitted by a metamaterial as discussed in Sec. V, the input states of light were vacuum states, which have a classical analogue (no light). By con-

$$\mathcal{S}_\sigma = \exp \left\{ \int_0^{\Delta\omega} d\omega [\xi_\sigma^*(\mathbf{k}, \omega) e^{-i\phi_{\sigma,\xi}(\mathbf{k}, \omega)} a_{\sigma,+}^{(1)\dagger}(\mathbf{k}, \omega) a_{\sigma,+}^{(1)\dagger}(\mathbf{k}, 2\Omega - \omega) - \text{h.c.}] \right\}, \quad (61a)$$

$$\mathcal{S}'_\sigma = \exp \left\{ \int_0^{\Delta\omega} d\omega [\zeta_\sigma^*(\mathbf{k}, \omega) e^{-i\phi_{\sigma,\zeta}(\mathbf{k}, \omega)} a_{\sigma,-}^{(N+1)\dagger}(\mathbf{k}, \omega) a_{\sigma,-}^{(N+1)\dagger}(\mathbf{k}, 2\Omega - \omega) - \text{h.c.}] \right\}. \quad (61b)$$

Here the $a_{\sigma,+}^{(1)}(\mathbf{k}, \omega)$ and $a_{\sigma,-}^{(N+1)}(\mathbf{k}, \omega)$ are the photonic annihilation operators of the incident fields with polarization σ and the transverse wave vector \mathbf{k} on the left- and right-hand sides of the multilayer slabs, respectively. It can be seen that the squeeze operators (61) correlate pairs of fixed-frequency modes on both sides of the frequency Ω . The amount of squeezing is controlled by the squeeze parameters $\xi_\sigma(\mathbf{k}, \omega)$ and $\zeta_\sigma(\mathbf{k}, \omega)$, which depend on the frequency, polarization, and angle of incidence. We specify the detector to be a balanced homodyne detector. It is well known that squeezing can be measured

in such a setup, where the signal field and a strong local oscillator are superimposed on a beam splitter, see Ref. [66] and the sketch in Fig. 6. The measured quantity is the difference in the photo currents of two detectors placed in the output arms of the beam splitter, as represented by the operator [65, 67]

We will consider the same metamaterial for which we calculated power spectra before, as detailed in Fig. 6. Since the tangential component \mathbf{k} is preserved under propagation through the multilayer and since there is air on both sides of the metamaterial, the output state of light will emerge from the loss-compensated multilayer at the same angle θ . Squeezing, specifically quadrature squeezing, occurs when the variance of the quantum fluctuations in one of the quadrature components of the electromagnetic field drop below the vacuum level. Squeezed states have no classical analogues and their non-classicality can be quantified by their associated normally ordered variances of the field operators [65]. Squeezed light can be produced by transmitting the radiation field through a nonlinear medium with a second-order nonlinearity $\chi^{(2)}$. Mathematically, the squeezed incident quantum states of light can be written as $|L\rangle = \mathcal{S}_\sigma|0\rangle$ and $|R\rangle = \mathcal{S}'_\sigma|0\rangle$, with squeeze operators belonging to a fixed in-plane wavevector \mathbf{k} given by

in such a setup, where the signal field and a strong local oscillator are superimposed on a beam splitter, see Ref. [66] and the sketch in Fig. 6. The measured quantity is the difference in the photo currents of two detectors placed in the output arms of the beam splitter, as represented by the operator [65, 67]

$$\hat{O}_\sigma = i \int_{t_0}^{t_0+T_0} dt \{ a_{\sigma,+}^{(N+1)\dagger} a_{\sigma,LO} - a_{\sigma,LO}^\dagger a_{\sigma,+}^{(N+1)} \}, \quad (62)$$

where on the right-hand side we suppressed the (\mathbf{k}, t) -

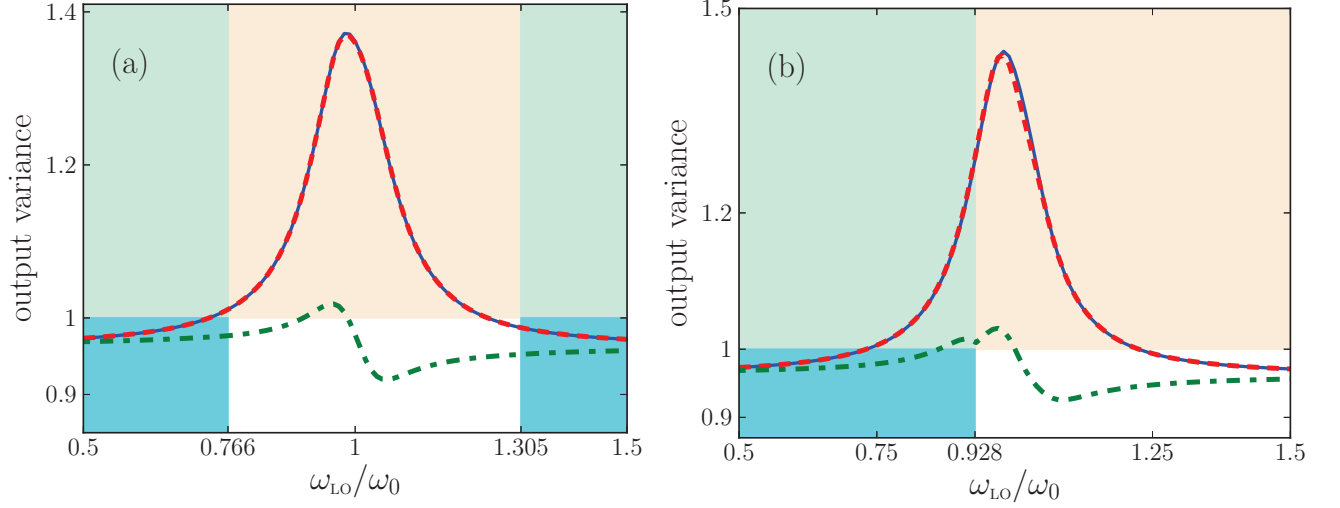


FIG. 7. (Color online) For squeezed light incident at an angle of $\theta = 30^\circ$ onto a loss-compensated multilayer metamaterial, a comparison of the predicted variances (64) as would be measured in balanced homodyne detection at a detection angle of also 30° . The metamaterial and the input states are described in Fig. 6. Predictions with exact multilayer theory (blue solid line) are compared with the quantum optical effective-index theory (green dash-dotted) and quantum optical effective-medium theory (red dashed), for s -polarized input states of light in panel (a) and for p -polarization in (b).

dependence of operators for readability. The detector is assumed to be polarization selective, and it is switched on from time t_0 to $t_0 + T_0$. The $a_{\sigma, \text{LO}}(t)$ and $a_{\sigma, \text{LO}}^\dagger$ are the creation and annihilation operators of the local-oscillator field with polarization σ . This local-oscillator field is assumed to be a single-mode coherent light beam represented by the complex amplitude $\alpha_{\sigma, \text{LO}}(t)$ that equals $F_{\text{LO}}^{1/2} \exp[-i(\omega_{\text{LO}}t - \phi_{\sigma, \text{LO}})]$, in terms of a flux F_{LO} , a phase $\phi_{\sigma, \text{LO}}$, and the frequency ω_{LO} . With the usual assumption that the local-oscillator field is much more intense than the signal field, the measurement operator \hat{O}_σ of Eq. (62) can be written as

$$\hat{O}_\sigma = F_{\text{LO}}^{1/2} \int_{t_0}^{t_0+T_0} dt E_\sigma(\phi_{\sigma, \text{LO}}, \mathbf{k}, t) \quad (63)$$

where the operator $E_\sigma(\phi_{\text{LO}}, \mathbf{k}, t)$ that equals $a_{\sigma, +}^{(N+1)}(\mathbf{k}, t) \exp[i(\omega_{\text{LO}}t - \phi_{\sigma, \text{LO}} - \pi/2)] + h.c$ is one quadrature operator of the output field with wave vector \mathbf{k} and polarization σ that exits the loss-compensated metamaterial on the right in Fig. 6. Balanced homodyne detection allows to measure a single quadrature component of the scattered field [66]. From the above definitions, the variance of the difference photocount in a narrow-bandwidth homodyne detector can be obtained

as [67, 68]

$$\begin{aligned} \langle [\Delta E_\sigma(\phi_{\sigma, \text{LO}}, \mathbf{k}, \omega_{\text{LO}})]^2 \rangle^{\text{out}} = & \quad (64) \\ 1 + 2 \langle a_{\sigma, +}^{(N+1)\dagger}(\mathbf{k}, \omega_{\text{LO}}), a_{\sigma, +}^{(N+1)}(\mathbf{k}, \omega_{\text{LO}}) \rangle & \\ + 2 \text{Re}[\langle a_{\sigma, +}^{(N+1)\dagger}(\mathbf{k}, \omega_{\text{LO}}), a_{\sigma, +}^{(N+1)\dagger}(\mathbf{k}, \omega_{\text{LO}}) \rangle e^{2i\phi_{\sigma, \text{LO}}}] & \end{aligned}$$

where the short-hand notation $\langle C, D \rangle \equiv \langle CD \rangle - \langle C \rangle \langle D \rangle$ has been introduced for a correlation. The scattered output state is squeezed if its photocount variance is smaller than that of the vacuum state value [65]. The homodyne electric-field operator has a variance (64) equal to unity for the vacuum state. Therefore, the amount of squeezing is gauged by the difference between this variance and unity. We will now calculate the quadrature variances in Eq. (64) in three ways: using the exact multilayer theory, the effective-index theory, and by the QOEM theory. In all three cases we make use of the commutation relation Eqs. (13) and the definition of the squeezing parameters (61). We start calculating the variances Eq. (64) with the multilayer theory, where the crucial relation between input and output operators is given by (38). This will result in rather long expressions, which is one of the reasons to try to find simple but accurate effective theories also in quantum optics. The two types of correlations in the variance in Eq. (64) are given by

$$\begin{aligned} \langle a_{\sigma, +}^{(N+1)\dagger}(\mathbf{k}, \omega), a_{\sigma', +}^{(N+1)}(\mathbf{k}', \omega') \rangle = \delta_{\sigma\sigma'} \delta(\mathbf{k} - \mathbf{k}') \delta(\omega - \omega') & (|\mathcal{A}_{\sigma, 22}(\mathbf{k}, \omega)|^2 \sinh^2 \xi_\sigma(\mathbf{k}, \omega) + |\mathcal{A}_{\sigma, 21}(\mathbf{k}, \omega)|^2 \sinh^2 \zeta_\sigma(\mathbf{k}, \omega)) \\ + \langle F_{\sigma, +}^\dagger(\mathbf{k}, \omega) F_{\sigma, +}(\mathbf{k}', \omega') \rangle, & \quad (65a) \end{aligned}$$

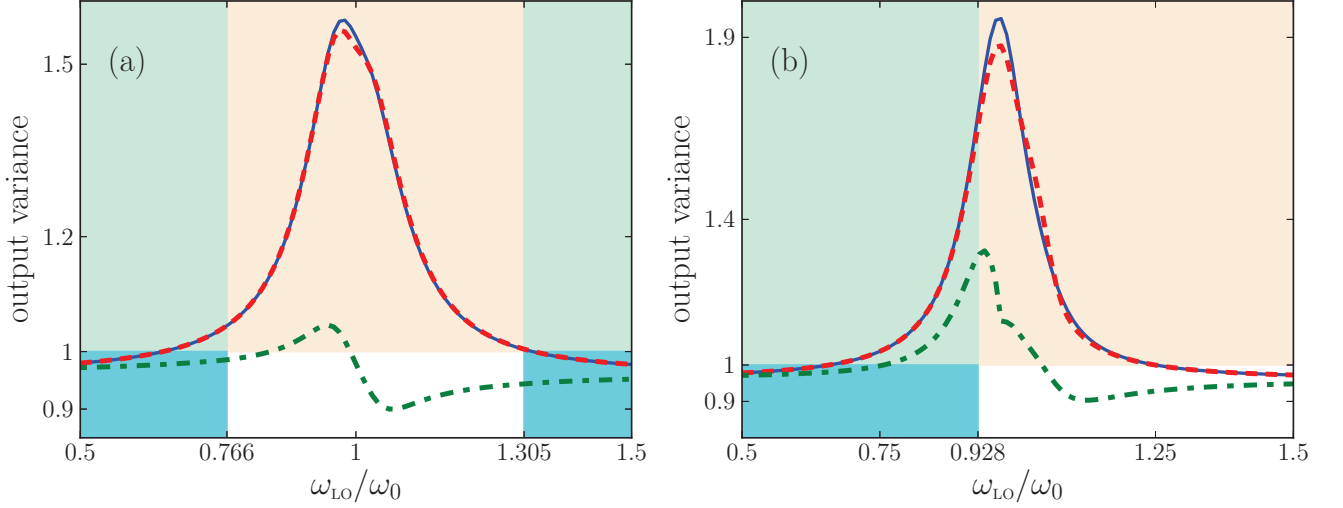


FIG. 8. Same as Fig. (7) but now for incident and detection angles of $\theta = 60^\circ$.

$$\begin{aligned} \langle a_{\sigma,+}^{(N+1)\dagger}(\mathbf{k}, \omega), a_{\sigma',+}^{(N+1)\dagger}(\mathbf{k}', \omega') \rangle &= \frac{1}{2} \delta_{\sigma\sigma'} \delta(\mathbf{k} - \mathbf{k}') \delta(\omega + \omega' - 2\Omega) \\ &\times \left(\mathcal{A}_{\sigma,22}^{*2}(\mathbf{k}, \omega) \sinh 2\xi_{\sigma}(\mathbf{k}, \omega) e^{-i\phi_{\sigma,\xi}(\mathbf{k}, \omega)} + \mathcal{A}_{\sigma,21}^{*2}(\mathbf{k}, \omega) \sinh 2\zeta_{\sigma}(\omega) e^{-i\phi_{\sigma,\zeta}(\mathbf{k}, \omega)} \right). \end{aligned} \quad (65b)$$

The homodyne signal depends on the noise as described by the operator $F_{\sigma,+}(\mathbf{k}, \omega)$, which represent the outgoing rightward-propagating noise field produced inside the multilayer medium. More specifically, the noise dependence is described by the expectation value $\langle F_{\sigma,+}^{\dagger}(\mathbf{k}, \omega) F_{\sigma,+}(\mathbf{k}', \omega') \rangle$, which is the same noise-photon flux that we also came across in the power spectrum (52). Thus the effect of the quantum noise on the squeezing properties of output light can be fully characterized by the emitted noise photons. The reason why only the first of these two expressions depends on the quantum noise is that the quantum noise is assumed to be in a thermal state for which $\langle F_{\sigma,+}^{\dagger}(\mathbf{k}, \omega) F_{\sigma,+}^{\dagger}(\mathbf{k}', \omega') \rangle$ vanishes.

We will compare predictions of the homodyne signal made with the exact multilayer theory and with the two effective theories. For the multilayer theory, we can insert into Eq. (65) the classical multilayer matrix $\mathcal{A}_{\sigma}(\mathbf{k}, \omega)$ of Eq. (40a) and the multilayer noise flux $\langle F_{\sigma,+}^{\dagger}(\mathbf{k}, \omega) F_{\sigma,+}(\mathbf{k}', \omega') \rangle_{\text{exact}}$ of Eq. (53) again. In both effective theories on the other hand, the exact matrix coefficients of the input-output matrix are to be replaced by the corresponding elements of the effective matrix \mathcal{A}_{eff} of Eq. (44). Furthermore, in the effective-index theory the noise photon flux is given by Eq. (55), while in the QOEM theory it is given by Eq. (57).

In Fig. 7 we compare the output squeezing spectrum predicted with the three theories, all for $T = 0$, at an angle of 30 degrees away from the normal. In Fig. 8 we show the same for an output angle of 60 degrees. For simplicity we take the squeezing strengths $\xi_{\sigma}^*(\mathbf{k}, \omega)$, $\zeta_{\sigma}^*(\mathbf{k}, \omega)$ and phases $\phi_{\sigma,\xi}$, $\phi_{\sigma,\zeta}$ to be constant in the depicted frequency

interval. We observe that the output squeezing spectrum is sensitive not only to the local-oscillator phase but also to the angle of incidence and the polarization. For this loss-compensated multilayer, the output squeezing spectrum shows a maximum exceeding unity in the vicinity of the resonance frequency. Noise photons destroy the squeezing property of the input field such that the output state will not at all be squeezed for most local-oscillator frequencies in the interval $[0.5\omega_0, 1.5\omega_0]$ shown in the figures. By contrast, in the same frequency interval the quantum optical effective-index theory predicts the output light to be squeezed for almost all local-oscillator frequencies. In other words, the output state of light of the loss-compensated material is considerably noisier than that of the homogeneous slab with the same β_{σ} . Thus Figs. 7 and 8 clearly illustrate the failure of the quantum optical effective-index theory for loss-compensated metamaterials. In Ref. 45 this failure was already established for normal incidence, and here we see that the agreement does not improve when detecting under an angle. The more important message from the figures is the very good agreement between the exact theory and QOEM effective theory, not only for normal incidence but also under an angle, and both for s - and for p -polarized light. Small numerical differences between the exact theory and the QOEM theory occur only close to resonance and only for large incident angles.

The colors of the frequency intervals in Figs. 7 and 8 label net loss and net gain, exactly as before in Figs. 2 and 3. When loss is exactly compensated by gain, we saw in these earlier figures that $N_{\text{eff},\sigma}(\mathbf{k}, \omega, T)$ diverges

while the output intensity was continuous. Here in Figs. 7 and 8 we see that likewise in homodyne detection the output variance is still continuous at those frequencies where $N_{\text{eff},\sigma}(\mathbf{k},\omega,T)$ diverges.

VIII. DISCUSSION AND CONCLUSIONS

We studied the propagation of quantum states of light through metamaterials, and showed that also in quantum optics an effective description of layered metamaterials can be given, for any angle of incidence and polarization. Quantum noise due to material loss or gain has an influence on the quantum states of light. We showed that in some situations the effective index suffices to describe the quantum noise, while in other cases an additional effective-medium parameter is needed, namely the effective noise-current density.

We tested our quantum optical effective-index theory (one effective parameter) and quantum optical effective-medium theory (two parameters) by calculating spectra and comparing with a full description of the multilayer metamaterial. For loss-compensated metamaterials, the gain regions emit noise photons, not described by the effective-index theory, that do affect the spectra. They have a similar effect on balanced homodyne detection measurements. We showed that our quantum optical effective-medium theory describes both the spectra and the homodyne signal well.

For normal incidence we found earlier that quantum noise of passive metamaterials can be described in terms of the effective index, and loss-compensated require the additional parameter. We now found that this also holds exactly for s -polarized light at all angles of incidence, but for p -polarized light the additional parameter is also needed for passive systems. For all angles of incidence and polarizations, we derived expressions for the new effective parameter.

Our results can be readily generalized to magnetic layered metamaterials. For metamaterials not composed of multilayers, more work would be needed to derive the effective noise current density. Metasurfaces with gain will similarly require a description in quantum optics that describes the quantum noise associated with the gain. Another interesting open question is whether the current effective-medium theories suffice to describe higher-order measurements, for example bunching or anti-bunching in intensity correlation measurements, for quantum states of light that propagated through metamaterials.

ACKNOWLEDGMENTS.

We thank N. Asger Mortensen for stimulating discussions and support. E.A. wishes to thank the Shahrekord University for support. M.W. gratefully acknowledges support from the Villum Foundation via the VKR Centre of Excellence NATEC-II and from the Danish Council

for Independent Research (FNU 1323-00087) The Center for Nanostructured Graphene is sponsored by the Danish National Research Foundation, Project DNR103.

Appendix A: Methods to obtain classical effective parameters

Scattering method.— The scattering method developed by Smith and coworkers [10, 11, 17] has proved extremely useful. The idea is to fit the scattering properties of a metamaterial by those of a homogeneous medium, with values for the effective parameters that give the best fit. Finding equivalent bulk parameters in this way is solving an inverse problem. Recently, this approach has been generalized to obliquely incidence [15] by assuming that the effective medium can be fully characterized by β_{eff} , the wave-vector component in normal direction (here: \hat{z} -direction). In fact, for oblique incidence, there is no need to introduce the effective refractive index because all details of wave propagation follow from this parameter β_{eff} . What is more, the refractive index may lose its physical meaning and may even become discontinuous, due to the branch cut of the complex square root [15, 69]. By retrieving the normal wave vector component β_{eff} from the reflection and transmission coefficients (45a) and (45b) of a homogenous medium with thickness L , the index of the plane wave for both polarizations s and p is derived as

$$\beta_{\text{eff},\sigma} L = \pm \arccos \left(\frac{1 - r_{\text{eff},\sigma}^2 + t_{\text{eff},\sigma}'^2}{2t_{\text{eff},\sigma}'} \right), \quad (\text{A1})$$

where $t_{\text{eff},\sigma}' = \mathcal{A}_{\sigma,21} \exp(i\beta_0 L)$ is the modified transmission amplitude. In general, the multiple branches associated with the inverse cosine of Eq. (A1) make the unambiguous determination of the normal wave vector component $\beta_{\text{eff},\sigma}$ difficult [17]. However, the ambiguity will not arise in our calculations since for simplicity we only consider situations where the wavelength within the medium is much larger than the multilayer length L .

Dispersion method.— Alternatively one can identify values for effective parameters using the dispersion method: the effective parameters of a periodic bi-layer system with permittivity functions $\varepsilon_a(\omega)$, $\varepsilon_b(\omega)$ and thicknesses $d_{a,b}$ are obtained from the Bloch dispersion relation

$$\begin{aligned} \cos(\beta_{\text{effb},s}d) &= \cos(\beta_a d_a) \cos(\beta_b d_b) \\ &\quad - \frac{1}{2} \left(\frac{\beta_{a,\sigma}}{\beta_{b,\sigma}} + \frac{\beta_{b,\sigma}}{\beta_{a,\sigma}} \right) \sin(\beta_a d_a) \sin(\beta_b d_b) \end{aligned} \quad (\text{A2})$$

in the long-wavelength limit. We describe s - and p -polarized light at the same time, since $\beta_{j,\sigma}$ stands for $\beta_{j,s} = \beta_j$ and $\beta_{j,p}$ for $\frac{\beta_j}{\varepsilon_j}$, while d equals the total thickness $d_a + d_b$ of the two bi-layers. By taking the Taylor expanding them near the point $(\omega, \mathbf{k}) = (0, \mathbf{0})$, we obtain

the dispersion relation

$$\frac{\beta_{\text{effb},\sigma}^2}{\varepsilon_{\text{eff},\sigma\parallel}} + \frac{k^2}{\varepsilon_{\text{eff},\sigma\perp}} = \frac{\omega^2}{c^2}, \quad (\text{A3})$$

in terms of two important effective parameters, namely $\varepsilon_{\text{eff},s\parallel} = \varepsilon_{\text{eff},p\parallel} = \varepsilon_{\text{eff},s\perp} = (\varepsilon_a d_a + \varepsilon_b d_b)/d$ and $\varepsilon_{\text{eff},p\perp} =$

$(\varepsilon_a \varepsilon_b d)/(\varepsilon_b d_a + \varepsilon_a d_b)$. These are standard effective dielectric tensor components that correspond to the direction of the electric field parallel (\parallel) and perpendicular (\perp) to the layers, respectively.

-
- [1] J. B. Pendry, *Negative refraction makes a perfect lens*, Phys. Rev. Lett. **85**, 3966 (2000).
- [2] V. M. Shalaev, *Optical negative-index metamaterials*, Nat. Photonics **1**, 41 (2007).
- [3] V. M. Shalaev, W. Cai, U. K. Chettiar, H.-K. Yuan, A. K. Sarychev, V. P. Drachev, and A. V. Kildishev, *Negative index of refraction in optical metamaterials*, Opt. Lett. **30**, 3356 (2005).
- [4] S. Anantha Ramakrishna and J. B. Pendry, *Removal of absorption and increase in resolution in a near-field lens via optical gain*, Phys. Rev. B **67**, 201101 (2003).
- [5] B. Wood, J. B. Pendry, and D. P. Tsai, *Directed subwavelength imaging using a layered metal-dielectric system*, Phys. Rev. B **74**, 115116 (2006).
- [6] W. Yan, N. A. Mortensen, and M. Wubs, *Hyperbolic metamaterial lens with hydrodynamic nonlocal response*, Opt. Express **21**, 15026 (2013).
- [7] T. Chen, S. Li, and H. Sun, *Metamaterials Application in Sensing*, Sensors **12**, 2742 (2012).
- [8] J. B. Pendry, Y. Luo, and R. Zhao, *Transforming the optical landscape*, Science **348**, 521 (2015).
- [9] D. J. Bergman, *The dielectric constant of a composite material – A problem in classical physics*, Phys. Rep. **43**, 377 (1978).
- [10] D. R. Smith, S. Schultz, P. Markoř, and C. M. Soukoulis, *Determination of effective permittivity and permeability of metamaterials from reflection and transmission coefficients*, Phys. Rev. B **65**, 195104 (2002).
- [11] D. R. Smith and J. B. Pendry, *Homogenization of metamaterials by field averaging (invited paper)*, J. Opt. Soc. Am. B **23**, 391 (2006).
- [12] O. Acher, J.-M. Lerat, and N. Malléjac, *Evaluation and illustration of the properties of metamaterials using field summation*, Opt. Express **15**, 1096 (2007).
- [13] S. Sun, S. Chui, and L. Zhou, *Effective-medium properties of metamaterials: A quasimode theory*, Phys. Rev. E **79**, 066604 (2009).
- [14] D. Felbacq, B. Guizal, G. Bouchitté, and C. Bourel, *Resonant homogenization of a dielectric metamaterial*, Microwave and Opt. Techn. Lett. **51**, 2695 (2009).
- [15] C. Menzel, C. Rockstuhl, T. Paul, F. Lederer, and T. Pertsch, *Retrieving effective parameters for metamaterials at oblique incidence*, Phys. Rev. B **77**, 195328 (2008).
- [16] A. Andryieuski, R. Malureanu, and A. V. Lavrinenko, *Wave propagation retrieval method for metamaterials: Unambiguous restoration of effective parameters*, Phys. Rev. B **80**, 193101 (2009).
- [17] N. A. Mortensen, M. Yan, O. Sigmund, and O. Breinbjerg, *On the unambiguous determination of effective optical properties of periodic metamaterials: a one-dimensional case study*, J. Eur. Opt. Soc. **5**, 10010 (2010).
- [18] G. T. Papadakis, P. Yeh, and H. A. Atwater, *Retrieval of material parameters for uniaxial metamaterials*, Phys. Rev. B **91**, 155406 (2015).
- [19] R. W. Ziolkowski, *Propagation in and scattering from a matched metamaterial having a zero index of refraction*, Phys. Rev. E **70**, 046608 (2004).
- [20] M. Silveirinha and N. Engheta, *Tunneling of electromagnetic energy through subwavelength channels and bends using ϵ -near-zero materials*, Phys. Rev. Lett. **97**, 157403 (2006).
- [21] B. Edwards, A. Alù, M. E. Young, M. Silveirinha, and N. Engheta, *Experimental verification of epsilon-near-zero metamaterial coupling and energy squeezing using a microwave waveguide*, Phys. Rev. Lett. **100**, 033903 (2008).
- [22] R. Sokhoyan and H. A. Atwater, *Quantum optical properties of a dipole emitter coupled to an ϵ -near-zero nanoscale waveguide*, Opt. Express **21**, 32279 (2013).
- [23] P. Moitra, Y. M. Yang, Z. Anderson, I. I. Kravchenko, D. P. Briggs, and J. Valentine, *Realization of an all-dielectric zero-index optical metamaterial*, Nature Phot. **7**, 791 (2013).
- [24] R. Maas, J. Parsons, N. Engheta, and A. Polman, *Experimental realization of an epsilon-near-zero metamaterial at visible wavelengths*, Nature Phot. **7**, 907 (2013).
- [25] S.-C. Jiang, X. Xiong, Y.-S. Hu, Y.-H. Hu, G.-B. Ma, R.-W. Peng, C. Sun, and M. Wang, *Controlling the polarization state of light with a dispersion-free metastructure*, Phys. Rev. X **4**, 021026 (2014).
- [26] J. Grgić, J. R. Ott, F. Wang, O. Sigmund, A.-P. Jauho, J. Mørk, and N. A. Mortensen, *Fundamental Limitations to Gain Enhancement in Periodic Media and Waveguides*, Phys. Rev. Lett. **108**, 183903 (2012).
- [27] J. Manzanares-Martinez, C. I. Ham-Rodriguez, D. Mectezuma-Enriquez, and B. Manzanares-Martinez, *Omnidirectional mirror based on Bragg stacks with a periodic gain-loss modulation*, AIP Adv. **4**, 017136 (2014).
- [28] I. D. Leon and P. Berini, *Modeling surface plasmon-polariton gain in planar metallic structures*, Opt. Express **17**, 20191 (2009).
- [29] P. Berini and I. De Leon, *Surface plasmon-polariton amplifiers and lasers*, Nat. Photonics **6**, 16 (2012).
- [30] S. Xiao, V. P. Drachev, A. V. Kildishev, X. Ni, U. K. Chettiar, H.-K. Yuan, and V. M. Shalaev, *Loss-free and active optical negative-index metamaterials*, Nature **466**, 735 (2010).
- [31] A. Boardman, V. Grimalsky, Y. Kivshar, S. Koshevaya, M. Lapine, N. Litchinitser, V. Malnev, M. Noginov, Y. Rapoport, and V. Shalaev, *Active and tunable metamaterials*, Laser Photonics Rev. **5**, 287 (2011).
- [32] *Active Plasmonics and Tuneable Plasmonic Metamaterials*, edited by A. V. Zayats and S. Maier (Wiley, Hoboken, NJ, 2013).

- [33] P. Jung, A. V. Ustinov, and S. M. Anlage, *Progress in superconducting metamaterials*, supercond. Sc. Techn. **27**, 073001 (2014).
- [34] M. S. Tame, K. R. McEnery, S. K. Ozdemir, J. Lee, S. A. Maier, and M. S. Kim, *Quantum plasmonics*, Nat. Phys. **9**, 329 (2013).
- [35] C. L. Cortes, W. Newman, S. Molesky, and Z. Jacob, *Quantum nanophotonics using hyperbolic metamaterials*, J. Opt. **14**, 063001 (2012).
- [36] M. Siomau, A. Kamli, S. A. Moiseev, and B. C. Sanders, *Entanglement creation with negative index metamaterials*, Phys. Rev. A **85**, 050303 (2012).
- [37] S. M. Wang, S. Y. Mu, C. Zhu, Y. X. Gong, P. Xu, H. Liu, T. Li, S. N. Zhu, and X. Zhang, *Hong-Ou-Mandel interference mediated by the magnetic plasmon waves in a three-dimensional optical metamaterial*, Opt. Express **20**, 5213 (2012).
- [38] D. Lu, J. J. Kan, E. E. Fullerton, and Z. Liu, *Enhancing spontaneous emission rates of molecules using nanopatterned multilayer hyperbolic metamaterials*, Nature Nanotech. **9**, 48 (2014).
- [39] P. K. Jha, X. Ni, C. Wu, Y. Wang, and X. Zhang, *Metasurface enabled remote quantum interference*, Phys. Rev. Lett. **115**, 025501 (2015).
- [40] T. Roger, S. Vezzoli, E. Bolduc, J. Valente, J. J. Heitz, J. Jeffers, C. Soci, J. Leach, C. Cousteau, N. I. Zheludev, and D. Faccio, *Coherent perfect absorption in deeply subwavelength films in the single-photon regime*, Nat. Commun. **6**, 7031 (2015).
- [41] M. A. al Farooqui, J. Breeland, M. I. Aslam, M. Sadatgol, Şahin K. Özdemir, M. Tame, L. Yang, and D. O. Güney, *Quantum entanglement distillation with metamaterials*, Opt. Express **23**, 17941 (2015).
- [42] M. Asano, M. Bechu, M. Tame, Şahin Kaya Özdemir, R. Ikuta, D. O. Güney, T. Yamamoto, L. Yang, M. Wegener, and N. Imoto, *Distillation of photon entanglement using a plasmonic metamaterial*, Sci. Rep. **5**, 18313 (2015).
- [43] J. Zhang, M. Wubs, P. Ginzburg, G. Wurtz, and A. V. Zayats, *Transmission quantum optics: designing spontaneous emission using coordinate transforms*, J. Opt. **18**, 044029 (2016).
- [44] Z.-Y. Zhou, D.-S. Ding, B.-S. Shi, X.-B. Zou, and G. C. Guo, *Characterizing dispersion and absorption parameters of metamaterial using entangled photons*, Phys. Rev. A **85**, 023841 (2012).
- [45] E. Amooghorban, N. A. Mortensen, and M. Wubs, *Quantum optical effective-medium theory for loss-compensated metamaterials*, Phys. Rev. Lett. **110**, 153602 (2013).
- [46] W. Yan, M. Wubs, and N. A. Mortensen, *Hyperbolic metamaterials: nonlocal response regularizes broadband supersingularity*, Phys. Rev. B **86**, 205429 (2012).
- [47] Z. Jacob, J.-Y. Kim, G. V. Naik, A. Boltasseva, E. E. Narimanov, and V. M. Shalaev, *Engineering photonic density of states using metamaterials*, Applied Physics B **100**, 215 (2010).
- [48] A. N. Poddubny, P. A. Belov, and Y. S. Kivshar, *Spontaneous radiation of a finite-size dipole emitter in hyperbolic media*, Phys. Rev. A **84**, 023807 (2011).
- [49] O. Kidwai, S. V. Zhukovsky, and J. E. Sipe, *Effective-medium approach to planar multilayer hyperbolic metamaterials: strengths and limitations*, Phys. Rev. A **85**, 053842 (2012).
- [50] B. Huttner and S. M. Barnett, *Quantization of the electromagnetic field in dielectrics*, Phys. Rev. A **46**, 4306 (1992).
- [51] B. Huttner and S. M. Barnett, *Dispersion and loss in a Hopfield dielectric*, Europhys. Lett. **18**, 487 (1992).
- [52] T. Gruner and D.-G. Welsch, *Quantum-optical input-output relations for dispersive and lossy multilayer dielectric plates*, Phys. Rev. A **54**, 1661 (1996).
- [53] M. Wubs and L. G. Suttorp, *Transient QED effects in absorbing dielectrics*, Phys. Rev. A **63**, 043809 (2001).
- [54] L. G. Suttorp and M. Wubs, *Field quantization in inhomogeneous absorptive dielectrics*, Phys. Rev. A **70**, 013816 (2004).
- [55] R. Matloob, R. Loudon, M. Artoni, S. M. Barnett, and J. Jeffers, *Electromagnetic field quantization in amplifying dielectrics*, Phys. Rev. A **55**, 1623 (1997).
- [56] S. Scheel, L. Knöll, and D.-G. Welsch, *QED commutation relations for inhomogeneous Kramers-Kronig dielectrics*, Phys. Rev. A **58**, 700 (1998).
- [57] E. Amooghorban, M. Wubs, N. A. Mortensen, and F. Kheirandish, *Casimir forces in multilayer magnetodielectrics with both gain and loss*, Phys. Rev. A **84**, 013806 (2011).
- [58] R. J. Glauber, in *Frontiers in Quantum Optics*, edited by E. R. Pike and S. Sarkar (Hilger, Bristol, 1986).
- [59] C. W. Gardiner and P. Zoller, *Quantum Noise*, 3rd ed. (Springer, Berlin, 2004).
- [60] M. S. Tomaš, *Green function for multilayers: light scattering in planar cavities*, Phys. Rev. A **51**, 2545 (1995).
- [61] J. Skaar, *On resolving the refractive index and the wave vector*, Opt. Lett. **31**, 3372 (2005).
- [62] J. Skaar, *Fresnel equations and the refractive index of active media*, Phys. Rev. E **73**, 026605 (2006).
- [63] B. Nistad and J. Skaar, *Causality and electromagnetic properties of active media*, Phys. Rev. E **78**, 036603 (2008).
- [64] J. Cresser, *Theory of the spectrum of the quantised light field*, Phys. Rep. **94**, 47 (1983).
- [65] K. J. Blow, R. Loudon, S. J. D. Phoenix, and T. J. Shepherd, *Continuum fields in quantum optics*, Phys. Rev. A **42**, 4102 (1990).
- [66] U. Leonhardt, *Measuring the Quantum State of Light* (Cambridge University Press, Cambridge, UK, 1997).
- [67] M. Artoni and R. Loudon, *Propagation of nonclassical light through an absorbing and dispersive slab*, Phys. Rev. A **59**, 2279 (1999).
- [68] D. Y. Vasylyev, W. Vogel, G. Manzke, K. Henneberger, and D.-G. Welsch, *Nonclassicality of radiation fields propagating in complex material systems*, Phys. Status Solidi B **246**, 293 (2009).
- [69] C. Rockstuhl, C. Menzel, T. Paul, T. Pertsch, and F. Lederer, *Light propagation in a fishnet metamaterial*, Phys. Rev. B **78**, 155102 (2008).